Chapter 2
Permian – Triassic Magmatic Activity in the Song Da Structure

Abstract Late Permian mafic-ultramafic volcanic and sub-volcanic rocks in the Song Đa Rift include four different associations in terms of low-Ti and high-Ti types. Low-Ti, high-Mg volcanic and sub-volcanic rocks are composed of komatiite, komatiitic basalt and basalt and are divided into three groups according to their petrological and geochemical features. Chemical composition of rocks of the komatiite-basalt association is alkali-low (but rather Na-high), very Ti-low, varying from Al-high komatiite to Al-low basalt. They are characterized by high content of Mg, Al, Ni, Co, Cu and Cr, and low of Ti, Fe, Na, K, P, Rb, Ba, Sr, Nb, Ta, Nd, Hf, Zr and REE. In general, based on geochemical and isotopic characteristics the Song Đa mafic-ultramafic rocks of the komatiite-basalt association may be products of a melt derived from depleted mantle suffering the impact of mantle plume. Digital modeling showed that the initial melt composition was correspondent to komatiitic basalt. Eruption ages of the magmas are 257 ± 24 Ma (by Rb/Sr age dating), and 270 ± 21 Ma (by Re/Os age dating).

High-Ti basalts (and picrite) and gabbro-dolerites are widely distributed in marginal areas as well as in the center of the Song Đa Rift and belong to three associations: andesite-basalt, andesite-picrite-basalt and trachybasalt-trachyandesite-trachydacite. The chemical compositions of high-Ti basalts are characterized by having high Ti content, moderately low Al, medium to low Mg, relatively low alkalinity, but high K, high Rb, Sr, Zr and LREE, but Nb and Ta varies from low- to hight. The high-Ti basalts have relatively restricted ranges of $(^{87}Sr/^{86}Sr)_i$ (0.7048–0.7079) and ƐNd(t) values (−5.7 to +3.1) indicating weak lithospheric signature that may be related to their trace element-rich nature and this is consistent with abundant earlier studies suggesting that the high-Ti basalts at Song Da or elsewhere in the ELIP formed from low degrees of partial melting.

T.-H. Tran et al., *Intraplate Magmatism and Metallogeny of North Vietnam*, Modern Approaches in Solid Earth Sciences 11,
DOI 10.1007/978-3-319-25235-3_2

2.1 Song Da Permian – Triassic Mafic and Ultramafic Pluton – Volcanic Formations

2.1.1 Magma Classification

Intracontinental rifting in northwest – southeast direction was commonly developed in Southeast Asia during the Permian – Triassic (Gatinsky 1986; Khain and Balukhovsky 1993; Metcalfe 1996). The activity was accompanied by strong ultramafic – mafic magmatism. The Song Da rift is located between the Ailao Shan – Red River shear zone to the northeast and the Song Ma suture zone in the southwest. Although rifting structure features in an intracontinental setting are well described and defined (Gatinsky and Thuc 1982; Toat 1987; Hoa 1995; Polyakov et al. 1996, and references therein) the formation and evolution of this rifting structure is a focus of hotly debate in many geological forums.

The Song Da rift, according to up-to-date geological concerns, includes other structural facies such as Son La, Song Da, Ninh Binh and part of Thanh Hoa zone in the tectonic scheme presented by Dovjikov (1965). There are a number of areas and ultramafic – mafic magmatic associations in this structure such as Cam Thuy, Vien Nam – Ba Vi, Kim Boi – Hoa Binh, Son La Pass, Bac Yen – Van Yen, Deo Chen (Chen Pass), Nam Muoi, Nam So and Sin Ho (Fig. 2.1).

The classification of Permian – Triassic ultramafic – mafic magmatic rocks in northwestern Vietnam have been done in a number of igneous studies; however, up to the present the matter is not conclusive. Based on the petrology, recent studies have shown that the Permian mafic and ultramafic volcanic rocks may be divided into two distinct complexes, e.g., Cam Thuy (P_3) and Vien Nam (P_3). These are described in the monograph 'Geological stratigraphic divisions of Vietnam' edited by Tong Dzuy Thanh and Vu Khuc (2005). However, due to lack of radiometric age data the above division may be inappropriate in terms of geochemical compositions of the magmatic associations. The Cam Thuy volcanic rocks comprises mostly homogeneous high – Ti basalt and andesitic basalt (andesite – basalt association); while volcanic (and sub-volcanic) rocks in the Vien Nam complex are geochemically heterogeneous that include both high- and low- Ti mafic and ultramafic types. Among the high- Ti mafic magmas (mostly basalt) of Vien Nam complex there are two distinct magmatic associations picrite – andesite – basalt (Nam So type) and trachybasalt – trachyandesite – trachydacite (Nam Muoi – Suoi Chat type) (Hoa 2002). In general, among the magmas in Vien Nam complex aside from ultramafic – mafic rock types termed as komatiite – basalt association volcanic and sub-volcanic subalkaline felsic rocks are also common (Polyakov et al. 1991, 1996; Phuong 1994). Sources to form the high- and low- Ti magmas in the Song Da structure are obviously different: the low-Ti magma was formed by melting of MORB-like depleted mantle, whereas the high- Ti type was produced by melting of an enriched mantle (Hoa 2002, 2005, 2007). Therefore, classifying both the magmas to a single formation may not be appropriate. Based on the geochemical characteristics the magmas in these areas may belong to two series, e.g., low- and high- Ti where the high-Ti is dominant (Hoa et al. 1998; Hoa 2002). On the other hand, mineralogical

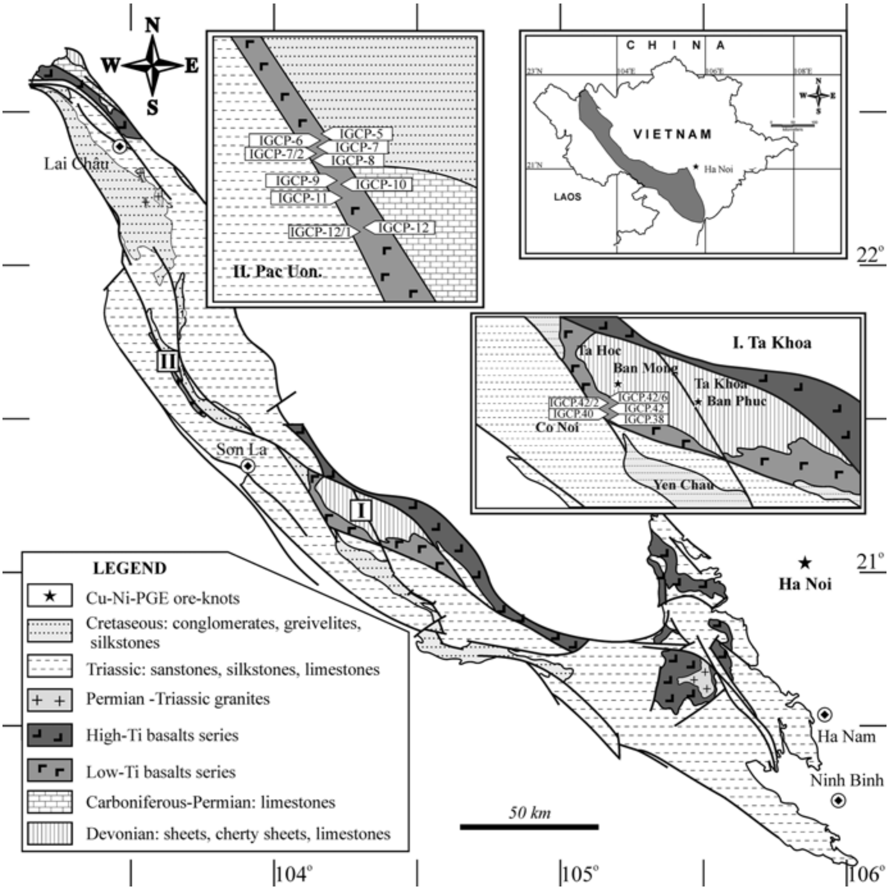

Fig. 2.1 Distribution scheme of Permian – Triassic magmatic formations within the Song Da structure

and geochemical studies (e.g. Polyakov et al. 1991, 1996; Hoa et al. 1998; Hoa 2002, 2005) distinguish the ultramafic – mafic rocks in the Song Da structure into various magmatic associations:

- Low-Ti series: including komatiite – basalt associations distributed in the center of Song Da rift, in the Nam Muoi and Ta Khoa areas.
- High-Ti series: with two different volcanic associations, one in the southeast and the other to the northwest along the alignment of Song Da zone. In the southeast andesite – basalt (and rhyolite – basalt) association is widely observed sometimes with a minor amount of sub-alkaline felsic (rhyodacite and rhyolite) rock types. These rock associations occur in the areas of Cam Thuy, Kim Boi, Vien Nam – Ba Vi, and Bac Yen – Van Yen. In contrast, in the northwest, the following volcanic associations are well-spread: andesite – basalt (Son La), picrite – andesite – basalt (Nam So) and trachydacite – trachyrhyolite – trachybasalt. Except for sub-alkaline volcanic rocks in the Nam Muoi area which is at the center of Song Da structure the other magmatic associations are distributed at the margins of this structure.

The formation ages of the Song Da ultramafic – mafic pluton-volcanic magmas are subjects to clarify. Age of the komatiite – basalt magmas in the Nam Muoi area was dated to be Permian – Triassic based on stratigraphic correlation and radiometric determination (Polyakov et al. 1991, 1996). Basaltic and komatiitic lavas in the Nam Muoi area are, on the one hand, overlain by carbonate terrigenous (shale) containing late Triassic fossils, and on the other, komatiitic subvolcanic bodies in the Nam Muoi and Ta Khoa areas penetrate Carboniferous and Permian terrigenous sediments. These observations were also reported by Pham Duc Luong (2005). Radiometric age dating (Rb-Sr) conducted on a basaltic komatiite (MgO = 18 wt%) yielded a value of 257 ± 24 Ma (Hoa 1995; Polyakov et al. 1996) (Fig. 2.2a). Re-Os age dating on 12 komatiite samples in the Nam Muoi area yielded a number of 270 ± 21 Ma (Hanski et al. 2004); Nguyen Hoang et al. (2004) reported a Rb-Sr age for Doi Bu high- Ti basalts at 280 Ma and 256 Ma for trachytes. Except for the age of 280 Ma that must be independently checked, other reported age data for the Song Da ultramafic – mafic magmas are rather consistent and closely similar to the reported eruption age of Emeishan basalts. Emeishan magmas aged about 260 Ma were thought to erupt within a short time span, from one to two million years (Zhong et al. 2007).

2.1.2 Komatiite – Basalt Associations in Nam Muoi and Ta Khoa Areas

2.1.2.1 Spatial Distribution Characteristics and Geological Structure

Up to date Song Da Rift high-Mg, low-Ti and low-alkali komatiite – basalt rocks have been convincingly defined in the two following areas Nam Muoi (Polyakov et al. 1991, 1996; Phuong 1994) and Ta Khoa (Hoa 1995) and more evidence was subsequently added later (e.g. Hoa 2005, 2007).

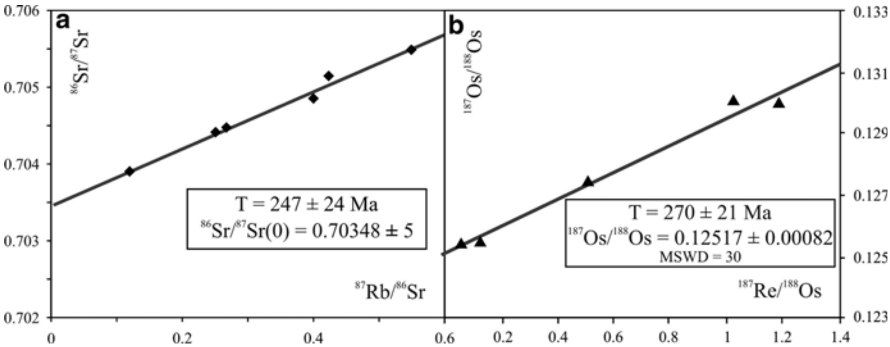

Fig. 2.2 Rb – Sr and Os – Re age dating for komatiitic basalt in the Nam Muoi area, (**a**) after Hoa 1995; Polyakov et al. 1996) and (**b**) after Hanski et al. 2004

Photo 2.1 Stratified structure between komatiite and low-Ti basalt. Outcrop nearby Pa Uon bridge cross Da river (By Hoa et al. 2013)

In the Nam Muoi area, high-Mg volcanic and sub-volcanic ultramafic – mafic rocks are described in two cross-sections Pac Uon- Muong Giang and Chieng Ngam (Fig. 2.1). In both two cross-sections bi-compositional, lower and upper, structures were defined. The lower structure is thicker and comprised of high-Mg volcanic rocks (olivine basalt, komatiitic basalt) and small bodies of pluton-volcanic ultramafic rocks. The upper unit the komatiitic basalt magma is replaced by sub-alkaline high-Ti mafic – felsic volcanic rock, a component of trachyandesite – trachydacite – trachybasalt association (Fig. 2.1, Photo 2.1).

In the Ta Khoa area high-Mg komatiitic basalts and peridotitic komatiites are distributed mainly to the southwest wing of the Ta Khoa anticline, in a shape of elongated lens, running in the northwest-southeast direction from Ta Hoc-Nong Xang in the northwest to Ban Tang village in the southeast. In difference to volcanic strata in the Nam Muoi area, accompanying Ta Khoa olivine basalt and komatiitic basalt are doleritic dykes, sometimes sub-volcanic komatiitic bodies. These sub-volcanic bodies appear either as conform lenses among the leucobasalt or dykes that cut through metamorphosed quartzite and mica shale. The most representative cross-section containing a variety of volcanic, sub-volcanic and plutonic komatiite – basalt association in the Ta Khoa area is Co Noi- Deo Chen – Ta Khoa. Olivine basalt, basalt with spinifex pyroxene, leucobasalt (andesitic basalt) and komatiitic and komatiitic peridotite sub-volcanic bodies may be observed long this cross-section (Photo 2.2).

In northwestern wing of the Ta Khoa anticlinorium, aside from volcanic and sub-volcanic rocks as mentioned above commonly observed are small-sized ultramafic bodies (dunite, lherzolite and pyroxenite) and dykes having compositions and structures similar to komatiic peridotite and olivine-bearing pyroxenite. In the Nam Chin area also encountered are zoned dykes comprising komatiic peridotite and olivine-bearing pyroxenite in the center and doleritic mafic magma in the marginal zone.

Photo 2.2 Komatiite lenses in low-Ti basalt in the Deo Chen area

PGE bearing Ni-Cu mineralization forming mid- (Ban Phuc) to small-sized industrial deposits (Ban Mong) are associated with these intrusive bodies and dykes.

Komatiite – Basalt associations in the Nam Muoi and Ta Khoa areas are distributed in the center of the Song Da structure. According to Bùi Minh and Tô Văn (1995) hi-Mg basalt of komatiite – basalt association also occurred in the Sin Ho area, northwest edge of the Song Da rift (Bùi Minh and Tô Văn 1995). Olivine basalt, a typical representative of the komatiite – basalt association (e.g. hi-Mg and low-Ti) is also observed in the Hoa Binh hydro-reservoir area as well as in the Doi Bu area. These volcanic rocks may be members comparable with those sub-volcanic magmas of Ba Vi-type. This suggestion needs further investigation to clarify. The Doi Bu and Hoa Binh hi-Mg and low-Ti volcanic rocks are not described in this monograph.

2.1.2.2 Petrographic and Mineralogical Characteristics

The hi-Mg (low-Ti series) volcanic rocks are classified into different groups according to their petrographic and geochemical characteristics. The first group includes ultramafic magmas having composition, structure and texture features similar to plagioclase-bearing wehrlite (MgO >30 wt.%), comprising coarse-grained olivine and a minor amount of pyroxene and plagioclase. These are the major component of the small sub-volcanic-like intrusive bodies occurred in komatiite – basalt volcanic layers in the Nam Muoi area, and among the small peridotite intrusive bodies (dunite, lherzolite) in the Ta Khoa area.

The second group includes magmas that show a chemical composition correspondent to komatiite (MgO = 22–30 wt.%) and occur in the form of sub-volcanic bodies as well as porous pillow-lavas in the Nam Muoi area. In the Ta Khoa area, these magma types are major constituents of sub-volcanic bodies in the Deo Chen volcanic cross-section. The magmas also occur as dykes in Nam Chim, Ta Hoc, and

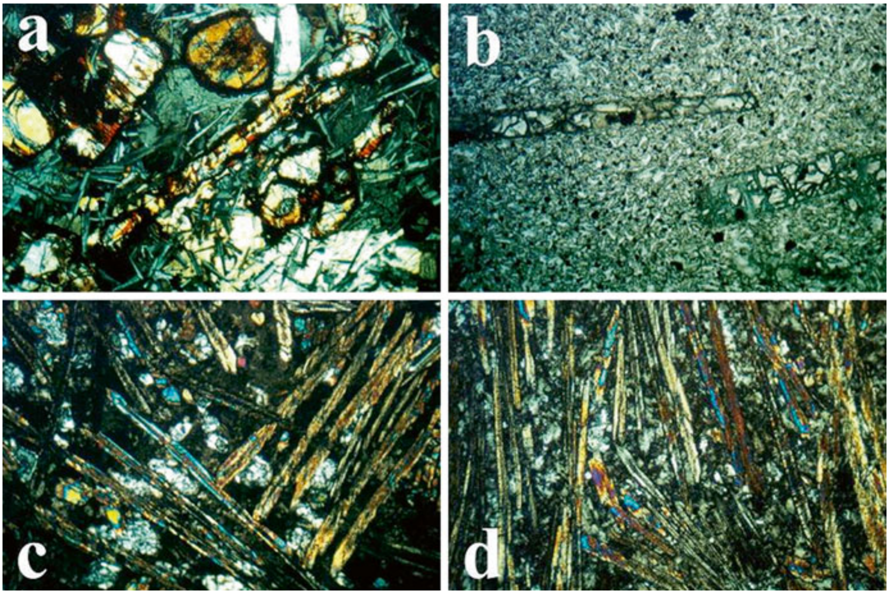

Photo 2.3 Porphyry (**a–b**) and spinifex (**c–d**) texture of pyroxene in Nam Muoi komatiitic basalt (After Polyakov et al. 1996)

Ban Mong areas. Most typical characteristics of this second group are that the mafic and ultramafic rocks show porphyry or porphyritic texture having elongated olivine phenocryst, and needle-shaped, spinifex-structured pyroxene (Polyakov et al. 1991) (Photo 2.3a–d).

The third group includes olivine basalt, olivine-free basalt, and transitional to andesitic basalt type. The olivine basalt and komatiitic basalt show elongated olivine and pyroxene phenocrysts in the ground masses of different level of crystallization. Among the phenocrysts, nearly rounded or anhydral olivine and pyroxene are commonly observed.

In association with magmatic intrusion and dyke activities in the Ta Khoa area, PGE bearing Ni-Cu mineralization is frequently occurred where Ban Phuc mine and Ban Mong ore site are most representatives (Hoa 1995; Hoa et al. 1998; Poliyakov et al. 1996; Phuong et al. 2001).

Major phenocryst minerals in the komatiitic basalt pluton volcanic associations are olivine, clinopyroxene and plagioclase, and the minor minerals are Cr-spinel and ilmenite. Aggregates of sulfur, sulfurarsenide, native copper, and PGM are also commonly occurred. Evolutional trend from dunite, peridotite and komatiite to olivine basalt is expressed by increasing the iron oxide in olivine from forsterite to chrysolite, decreasing the calcium oxide from bytownite to andesine in plagioclase, increasing the iron oxide in clinopyroxene and the Ti-, Fe- contents in Cr-spinel (Polyakov et al. 1996) (Tables 2.1, 2.2, 2.3 and 2.4). In general, mineralogical compositions of the komatiitic basalt associations of Song Da structure are closely

Table 2.1 Chemical compositions of olivine in komatiite and komatiitic basalt in the Nam Muoi and Ta Khoa areas. (EPMA analysis conducted at the Analytical Center, Institute of Geology and Mineralogy, Siberian Branch, Russian Academy of Sciences)

Sample ID	FeO	MgO	CaO	NiO	Ni (ppm)	f(*)
Nam Muoi						
Komatiite						
B6822	12.62	46.24	0.3	0.32	2476	13.3
B6825	8.1	49.03	0.27	0.4	3129	8.5
B6834	13.24	45.08	0.31	0.31	2437	14.1
B6854	11.87	46.25	0.29	0.33	2608	12.6
B6859	11.64	46.75	0.33	0.32	2476	12.3
B6860	12.06	46.5	0.23	0.3	2358	12.9
B6875	13.67	45.08	0.3	0.33	2608	14.5
B6885	13.54	44.79	0.34	0.3	2358	14.5
B7310	8.83	48.59	0.57	0.38	2985	9.3
B7329	12.27	46.91	0.37	0.35	2759	12.8
P250	11.36	46.58	0.36	0.27	2130	12
P260	12.88	45.16	0.32	0.24	1893	13.8
G1435	12.69	45.45	0.33	0.29	2278	13.1
G1441	12.65	45.22	0.3	0.33	2608	13.5
G1442	12.45	45.82	0.34	0.31	2437	13
G1444	12.49	46.07	0.33	0.29	2278	13.2
G1452	12.53	46.12	0.3	0.34	2670	13.2
G1453	18.51	40.77	0.32	0.26	2028	20.3
G1458	14.52	43.55	0.52	0.27	2130	15.8
G1461	12.52	43.25	0.27	0.33	2608	13.2
1/86	11.7	46.1	0.35	0.3	2358	12.5
9/86	13.44	45.22	0.33	0.3	2358	14.3
15/86	11.84	46.19	0.29	0.35	2759	12.5
34c/86	12.39	46	0.29	0.31	2437	13.2
43/86	12.55	45.91	0.32	0.32	2476	13.2
48a/86	11.64	46.55	0.32	0.3	2358	12.4
Pyroxenite						
B6842	14.38	44.2	0.3	0.31	2437	15.4
B6865	11.85	46.23	0.34	0.33	2608	12.6
B6888	13.17	45.14	0.31	0.29	2278	14.1
B6890	12.04	46.26	0.3	0.32	2476	12.7
B6892	13.62	44.88	0.35	0.27	2130	14.6
P272	8.1	49.33	0.28	0.3	2358	8.4
G1448	11.7	46.87	0.27	0.36	2812	12.3
G1456	11.49	46.49	0.3	0.31	2437	12.2

(continued)

Table 2.1 (continued)

Sample ID	FeO	MgO	CaO	NiO	Ni (ppm)	f(*)
7/86	8.17	49.5	0.26	0.41	3218	8.5
8/86	8.29	49.41	0.27	0.39	3074	8.6
33a/86	16.37	43	0.31	0.25	1987	17.8
48b/86	11.65	45.86	0.31	0.32	2476	12.5
Basalt- komatiite						
B6821	10.63	47.36	0.3	0.36	2812	11.2
B6830	12.29	46.48	0.33	0.34	2670	13
B6871	12.74	46.02	0.3	0.31	2437	13.4
B6889	12.53	45.26	0.32	0.29	2278	13.5
B6891	11.58	46.5	0.3	0.32	2476	12.3
Nam Muoi						
P247	16.96	42.16	0.33	0.12	943	18.4
48c/86	11.19	46.58	0.3	0.36	2812	11.8
G944	7.53	51.4	0.32	0.38	2985	7
48/86	12.13	45.54	0.32	0.32	2476	13
Ta Khoa						
T1631	11.28	46.09	0.26	0.38	2985	12
T1645	11.86	46.99	0.32	–	–	12
T1646-1	12.98	46.88	0.2	–	–	13

(*) ferrous content, $f = 100 \times FeO/(FeO + MgO)$

Table 2.2 Chemical compositions of pyroxene in komatiite and komatiitic basalt in the Nam Muoi and Ta Khoa areas

	Nam Muoi						Ta Khoa	
Sample ID	P67	B7329	B7335	P131Á/89	B7310	B7243	B5213	T1638
SiO_2	52.40	52.7	50.36	48.15	50.36	48.23	51.16	51.65
TiO_2	0.33	0.39	0.44	1.2	0.96	1.56	0.63	0.39
Al_2O_3	4.08	1.78	3.52	5.5	3.64	4.90	3.33	3.21
Cr_2O_3	0.11	0.17	0.28	0.12	0.23	0.01	0.77	0.01
FeO	6.61	7.32	7.6	9.29	10.21	9.71	6.83	12.34
MgO	18.18	18.68	16.92	14.77	14.97	12.25	17.78	13.65
CaO	17.39	18.05	19.72	19.89	19.35	22.35	18.15	16.70
Na_2O	0.13	0.25	0.37	0.34	0.26	0.48	0.26	0.54
Total	99.23	99.34	99.21	99.26	99.98	99.49	98.91	98.49
f	17	18	20.6	26	27.7	30.7	17.7	33.7
Wo.%	36.3	36.3	40.8	41.7	40.1	47.6	38.4	44.8
En.%	52.9	52.3	47.8	43.1	43.3	36.3	52.5	39.4
Fs.%	10.8	11.4	12.1	15.2	16.6	16.1	9.1	15.8

Table 2.3 Chemical compositions of plagioclase in komatiite and komatiitic basalt in the Nam Muoi and Ta Khoa areas

Sample ID	SiO_2	Al_2O_3	FeO	CaO	Na_2O	K_2O	An. %	Ab. %	Or. %
Komatiite									
B6842	52.29	29.53	0.77	13.3	3.82	0.09	65.2	34.2	0.6
B6859	47.58	32.83	0.39	17.2	1.81	0.01	85.4	14.6	0
B6865	49.14	31.56	0.5	16.0	2.21	0.01	80.3	19.6	0.1
B6888	52.39	30.02	0.09	12.5	4.18	0.26	61.4	37	1.6
B7310	51.79	28.02	1.07	12.1	4.42	0.12	59.8	40	0.2
B7329	51.73	28.94	0.83	13.3	3.81	0.24	66.4	32	1.6
P260	47.99	33.3	0.05	16.3	2.17	0.03	81	19	
G1442	54.97	27.78	0.47	10.7	5.1	0.28	52	46.2	1.8
G1458	49.51	31.39	0.58	15.3	2.65	0.1	76	23.6	0.4
1/86	50.8	30.59	0.13	13.3	3.8	0.15	66	33	1
9/86	53.27	29.31	0.23	12.0	4.45	0.38	58.6	39	2.4
15/86	49.91	30.38	0.74	15.1	2.9	0.03	74.4	25.5	0.1
43/86	50.49	30.71	0.59	14.5	3.04	0.11	72.5	27	0.5
Pyroxenite									
B6842	52.29	29.53	0.77	13.3	3.82	0.09	65.2	34.2	0.6
B6865	49.14	31.56	0.5	16.0	2.21	0.01	80.3	19.6	0.1
B6888	52.39	30.02	0.09	12.5	4.18	0.26	61.4	37	1.6
P272	50.73	31.33	0.14	14.1	3.41	0.06	69.4	30.5	0.1
8/86	54.24	28.63	0.34	11.4	4.98	0.34	56.2	41.8	2
Basalt komatiite									
B6891	55.66	27.99	0.18	10.3	5.29	0.26	51.8	46.4	1.8
B7335	50.93	28.54	1.56	12.8	3.93	0.06	64.6	35.2	0.2
P247	50.45	31.52	0.12	14.3	3.22	0.05	71.2	28.6	0.2
Olivine basalt									
P129/89	49.26	30.3	1.41	14.6	2.88	0.05	72.8	26.8	0.4
P131A/89	49.13	29.7	1.67	14.5	2.93	0.08	72.4	26.6	1
P131B/89	53.45	27.68	1.01	10.8	5.07	0.08	53.6	45.8	0.6

similar to those typical type occurred elsewhere in the world, in that: (1) the plagioclase, showing range between labrador – bytownite, is poor in orthoclase component but relatively high FeO contents (up to 1.7 %); (2) the olivine, varying between forsterite and chrysolite ($Fo_{78–93}$), is rich in Ni and Ca (NiO =0.1–0.4 %; CaO =0.2–0.6 %); the clinopyroxene, showing composition between augite and diopside, is poor in Ca, Ti, Ba, and average Cr contents ($En_{36-53}Fs_{9-17}Wo_{36–48}$, TiO_2 = 0.21.56 %, Cr_2O_3 up to 0.3 %); 4) the Cr-spinel shows composition correspondent to low-Ti, Al-chromite (Cr_2O_3 = 34–51 %, Al_2O_3 = 17–31 %, TiO_2 = 0.3–0.6 %) (Polyakov et al. 1996; Phuong et al. 2001).

Table 2.4 Chemical compositions of Cr-spinel in komatiite and komatiitic basalt in the Nam Muoi and Ta Khoa areas

Sample ID	SiO_2	Al_2O_3	FeO	CaO	Na_2O	K_2O	An. %	Ab. %	Or. %
Komatiite									
B6842	52.29	29.53	0.77	13.3	3.82	0.09	65.2	34.2	0.6
B6859	47.58	32.83	0.39	17.2	1.81	0.01	85.4	14.6	0
B6865	49.14	31.56	0.5	16.0	2.21	0.01	80.3	19.6	0.1
B6888	52.39	30.02	0.09	12.5	4.18	0.26	61.4	37	1.6
B7310	51.79	28.02	1.07	12.1	4.42	0.12	59.8	40	0.2
B7329	51.73	28.94	0.83	13.3	3.81	0.24	66.4	32	1.6
P260	47.99	33.3	0.05	16.3	2.17	0.03	81	19	
G1442	54.97	27.78	0.47	10.7	5.1	0.28	52	46.2	1.8
G1458	49.51	31.39	0.58	15.3	2.65	0.1	76	23.6	0.4
1/86	50.8	30.59	0.13	13.3	3.8	0.15	66	33	1
9/86	53.27	29.31	0.23	12.0	4.45	0.38	58.6	39	2.4
15/86	49.91	30.38	0.74	15.1	2.9	0.03	74.4	25.5	0.1
43/86	50.49	30.71	0.59	14.5	3.04	0.11	72.5	27	0.5
Pyroxenite									
B6842	52.29	29.53	0.77	13.3	3.82	0.09	65.2	34.2	0.6
B6865	49.14	31.56	0.5	16.0	2.21	0.01	80.3	19.6	0.1
B6888	52.39	30.02	0.09	12.5	4.18	0.26	61.4	37	1.6
P272	50.73	31.33	0.14	14.1	3.41	0.06	69.4	30.5	0.1
8/86	54.24	28.63	0.34	11.4	4.98	0.34	56.2	41.8	2
Komatiitic basalt									
B6891	55.66	27.99	0.18	10.3	5.29	0.26	51.8	46.4	1.8
B7335	50.93	28.54	1.56	12.8	3.93	0.06	64.6	35.2	0.2
P247	50.45	31.52	0.12	14.3	3.22	0.05	71.2	28.6	0.2
Olivine basalt									
P129/89	49.26	30.3	1.41	14.6	2.88	0.05	72.8	26.8	0.4
P131A/89	49.13	29.7	1.67	14.5	2.93	0.08	72.4	26.6	1
P131B/89	53.45	27.68	1.01	10.8	5.07	0.08	53.6	45.8	0.6

2.1.2.3 Geochemical Characteristics

Chemical compositions of the komatiitic basalt associations are characterized by having low alkalis (but relatively high Na), very low Ti and by evolution trend from hi-Al komatiite to low-Al basalt. They are characteristically high Mg, Al, Ni, Co, Cr and low Ti, Fe, Na, K, P, Rb, Ba, Sr, Nb, Ta, Nd, Hf, Zr, REE (Table 2.5).

Primitive mantle normalized trace element (LILE, HFSE and REE) patterns (after Sun and McDonough 1989) show a weak differentiation among the elements whose concentrations exceed those of the primitive mantle from one to ten times (Fig. 2.3). The plagioclase basalts and serpentinized peridotites show relatively high Cr, Rb, U, La and Ce, while the peridotites, komatiites and komatiitic basalts have Th, Nb, Zr, Ba, Sr, Nd, Hf, Y and REE contents closely matching with the primitive mantle (e.g. Sun and McDonough 1989). These geochemical features are character-

Table 2.5 Chemical compositions (wt. %) and trace element contents in the low-Ti volcanic rocks in the Nam Muoi and Ta Khoa areas (Nam Muoi area, after Hanski et al. 2004)

Sample ID	IGCP-42	IGCP-42/1	IGCP-42/6	IGCP-38	IGCP-40
	Komatiite		Olivine basalt		Andesite
SiO_2	40.1	43.2	47.7	43.8	59.0
TiO_2	0.33	0.76	0.62	0.94	0.70
Al_2O_3	5.34	10.30	13.20	10.50	14.20
Fe_2O_3	9.85	10.38	9.21	11.98	7.04
MnO	0.14	0.17	0.14	0.19	0.12
MgO	29.10	15.90	8.45	12.50	4.28
CaO	4.46	10.04	12.93	11.14	7.56
Na_2O	0.00	0.99	1.78	1.94	1.83
K_2O	0.09	0.02	0.44	0.02	1.38
P_2O_5	0.07	0.17	0.07	0.20	0.08
CO_2	0.04	0.04	0.04	0.07	0.04
H_2O	9.39	4.71	2.49	4.47	2.48
V	131	209	214	277	171
Cr	3118	1516	509	965	102
Ni	1630	672	45	396	15
Cu	54	102	81	105	33
Zn	72	79	67	97	72
Ga	9	16	16	16	24
Sr	10	139	167	52	127
Zr	16	48	64	43	162
Ba	36	28	132	38	168
Pb	10	11	12	14	19
Bi	1	4	0	1	4
Ce	3.77	12.5	16.9	9.47	46.3
Dy	1.65	3.58	3.83	4.49	5.02
Er	1.23	2.49	2.75	2.51	3.78
Eu	0.51	1.03	0.82	1.09	1.26
Gd	1.6	3.3	3.82	3.23	5.5
Ho	0.38	0.96	0.77	0.83	1.27
La	1.82	6.05	7.98	4.51	21.8
Lu	0.35	0.66	0.45	0.72	0.55
Nd	4.23	8.45	10.8	9.09	23.4
Pr	0.7	1.98	2.35	1.54	5.48
Sm	1.53	3.56	2.7	4.18	5.55
Tb	0.39	0.57	0.54	0.74	0.9
Tm	0.33	0.51	0.51	0.61	0.65
Yb	1.35	3.4	3.03	3.58	3.51
Sc	22.7	37.5	34.1	51.2	28
Y	6.79	16.2	17.1	19.2	29.7

(continued)

Table 2.5 (continued)

Sample ID	IGCP-42	IGCP-42/1	IGCP-42/6	IGCP-38	IGCP-40
U	0.55	0.68	0.94	0.97	1.82
Th	0.69	2.37	3.04	1.96	7.83
Hf	1.18	2.16	2.49	2.35	3.88
Nb	2.25	8.04	4.59	7.18	8.84
Rb	9.56	1.36	7.11	1.39	29.3
Ta	0.3	0.71	0.46	0.74	0.86

Sample ID	IGCP-6	IGCP-5	IGCP-7	Sample ID	IGCP-6	IGCP-5	IGCP-7
Rock type	Komatiite		Basalt	Rock type	Komatiite		Basalt
SiO_2	41.50	45.50	46.60	Pb	12	16	9
TiO_2	0.55	0.61	1.01	Ce	1.93	2.16	7.03
Al_2O_3	9.48	9.55	14.40	Dy	3.02	2.86	6.23
Fe_2O_3	10.79	8.64	11.88	Er	2.11	1.78	3.51
MnO	0.15	0.14	0.19	Eu	0.78	0.73	1.6
MgO	20.80	12.30	8.30	Gd	2.55	2.5	4.91
CaO	7.60	14.25	9.55	Ho	0.6	0.57	1.3
Na_2O	0.56	0.38	2.54	La	0.76	0.47	2.77
K_2O	0.02	0.01	1.09	Lu	0.37	0.28	0.74
P_2O_5	0.03	0.03	0.11	Nd	3.85	3.72	7.54
CO_2	0.13	0.24	0.04	Pr	0.64	0.48	1.64
H_2O	5.50	5.61	2.60	Sm	2.54	2.03	4.41
S	0	0.0009	0	Tb	0.57	0.44	0.85
Cl	0.004	0.0042	0.0058	Tm	0.37	0.32	0.8
V	183	182	321	Yb	2	2	4
Cr	1890	961	397	Sc	31	31.9	45.2
Ni	1044	379	189	Y	13.5	15	25.3
Cu	105	51	513	U	0.55	0.22	0.76
Zn	73	71	89	Th	0.61	0.5	1.22
Ga	12	18	19	Hf	1.37	1.05	2.85
Sr	42	23	220	Nb	0.69	0.66	2.49
Zr	24	25	49	Rb	3.97	0.68	32.7
Ba	28	20	117	Ta	0.56	0.2	0.45

Sample ID	IGCP-6	IGCP-5	IGCP-7	Sample ID	IGCP-6	IGCP-5	IGCP-7
Rock type	Komatiite		Basalt	Rock type	Komatiite		Basalt
SiO_2	41.50	45.50	46.60	Pb	12	16	9
TiO_2	0.55	0.61	1.01	Ce	1.93	2.16	7.03
Al_2O_3	9.48	9.55	14.40	Dy	3.02	2.86	6.23
Fe_2O_3	10.79	8.64	11.88	Er	2.11	1.78	3.51
MnO	0.15	0.14	0.19	Eu	0.78	0.73	1.6
MgO	20.80	12.30	8.30	Gd	2.55	2.5	4.91
CaO	7.60	14.25	9.55	Ho	0.6	0.57	1.3
Na_2O	0.56	0.38	2.54	La	0.76	0.47	2.77

(continued)

Table 2.5 (continued)

Sample ID	IGCP-6	IGCP-5	IGCP-7	Sample ID	IGCP-6	IGCP-5	IGCP-7
K_2O	0.02	0.01	1.09	Lu	0.37	0.28	0.74
P_2O_5	0.03	0.03	0.11	Nd	3.85	3.72	7.54
CO_2	0.13	0.24	0.04	Pr	0.64	0.48	1.64
H_2O	5.50	5.61	2.60	Sm	2.54	2.03	4.41
S	0	0.0009	0	Tb	0.57	0.44	0.85
Cl	0.004	0.0042	0.0058	Tm	0.37	0.32	0.8
V	183	182	321	Yb	2	2	4
Cr	1890	961	397	Sc	31	31.9	45.2
Ni	1044	379	189	Y	13.5	15	25.3
Cu	105	51	513	U	0.55	0.22	0.76
Zn	73	71	89	Th	0.61	0.5	1.22
Ga	12	18	19	Hf	1.37	1.05	2.85
Sr	42	23	220	Nb	0.69	0.66	2.49
Zr	24	25	49	Rb	3.97	0.68	32.7
Ba	28	20	117	Ta	0.56	0.2	0.45

Sample	G1456	B6889	B6865	B6859	B6891	B6892	P12/86	P46/89	P8/86	P9/86	G1436
SiO_2	43.41	44.68	44.55	40.89	40.60	42.28	46.80	44.90	43.54	41.86	47.90
TiO_2	0.52	0.56	0.39	0.36	0.53	0.54	0.46	0.47	0.58	0.44	0.61
Al_2O_3	10.41	9.84	9.55	7.11	10.19	9.77	10.97	9.90	9.40	8.79	13.42
Fe_2O_3	11.78	11.54	10.85	11.02	11.12	12.04	8.49	11.23	11.52	11.57	9.54
MnO	0.17	0.17	0.17	0.16	0.16	0.17	0.16	0.16	0.17	0.17	0.15
MgO	20.78	22.08	22.60	27.44	21.05	22.37	11.39	21.36	22.13	24.85	8.20
CaO	8.17	8.57	8.77	6.55	7.90	8.80	15.25	8.04	7.39	7.09	12.88
Na_2O	0.85	0.99	0.77	0.10	0.95	0.61	0.44	0.77	0.70	0.33	2.76
K_2O	0.03	0.02	0.01	0.07	0.04	0.04	0.00	0.09	0.02	0.02	0.02
P_20_5	0.04	0.04	0.02	0.02	0.05	0.04	0.03	0.03	0.04	0.03	0.05
LOI	2.88	1.79	2.08	6.08	2.48	3.07	3.95	2.38	4.30	4.69	3.96
Total	99.05	100.28	99.76	99.80	99.06	99.73	97.94	99.33	99.79	99.83	99.47
Cr	2034	1930	2519	3022	1763	1844	3687	2072	1804	2575	316
Ni	926	908	971	1382	1030	908	313	1072	1099	1259	123
Co	79.7	80	79	92.5	77.3	74.4	42.6	75	80.7	87.8	36.1
Sc	36.1	32.9	33.3	28	33	34.6	38.4	34.9	28.7	24.6	42.1
V	193	222	200	141	185	193	221	181	178	152	251
Zr	21.3	21.9	12.8	11.1	20.9	22.3	14.9	17.2	23.6	15.2	28
Hf	0.78	0.67	0.38	0.5	0.64	0.64	0.59	0.59	0.83	0.56	0.91
Nb	0.69	0.64	0.43	0.33	0.6	0.57	0.74	0.52	0.45	0.47	1.26
Th	<0.5	0.076	0.040	<0.5	<0.5	<0.5	<0.5	<0.5	<0.5	<0.5	0.87
U	<0.2	0.020	0.014	<0.2	<0.2	<0.2	<0.2	<0.2	<0.2	<0.2	<0.2
Rb	5.02	1.35	1.20	2.85	3.06	1.39	0.08	5.99	3.05	1.81	0.52
Sr	39	43.3	29.7	27	57	47	18	35	41	71.4	72
Ba	19	5.17	6.56	23	29	16	33	23	21	25	27

(continued)

Table 2.5 (continued)

Sample	G1456	B6889	B6865	B6859	B6891	B6892	P12/86	P46/89	P8/86	P9/86	G1436
Y	13.9	12.5	8.8	8.5	14.2	14.1	12.4	11.5	12.5	9.8	16.5
Cu	89	101	85	76	88	82	148	105	95	85	141
Zn	80	69	65	67	72	76	70	90	78	73	78
La	0.7	0.64	0.36	0.49	1.24	0.68	<0.8	0.89	0.66	<1.0	2.91
Ce	2.08	0.2.05	1.18	1.12	3.20	2.03	1.57	2.00	2.05	2.39	6.51
Pr	0.33	0.39	0.22	0.20	0.50	0.38	0.27	0.31	0.40	0.35	0.82
Nd	2.25	2.37	1.36	1.34	2.70	2.34	1.61	1.69	2.45	1.82	4.00
Sm	0.99	1.11	0.35	0.51	1.08	1.07	0.71	0.72	1.01	0.71	1.22
Eu	0.38	0.48	0.30	0.22	0.47	0.45	0.32	0.32	0.49	0.33	0.51
Gd	1.78	1.84	1.12	1.03	1.79	1.93	1.32	1.46	1.74	1.25	1.90
Tb	0.31	0.36	0.23	0.19	0.33	0.36	0.25	0.24	0.32	0.24	0.36
Dy	2.39	2.33	1.58	1.37	2.23	2.35	1.77	1.79	2.17	1.67	2.47
Ho	0.49	0.53	0.37	0.31	0.51	0.51	0.41	0.40	0.45	0.37	0.58
Er	1.48	1.55	1.14	0.90	1.44	1.50	1.27	1.30	1.29	1.01	1.90
Tm	0.20	0.22	0.17	0.15	0.19	0.22	0.19	0.19	0.19	0.16	0.28
Yb	1.43	1.41	1.07	0.93	1.36	1.42	1.38	1.26	1.23	1.02	1.76
Lu	0.23	0.21	0.17	0.15	0.19	0.20	0.21	0.21	0.19	0.16	0.27

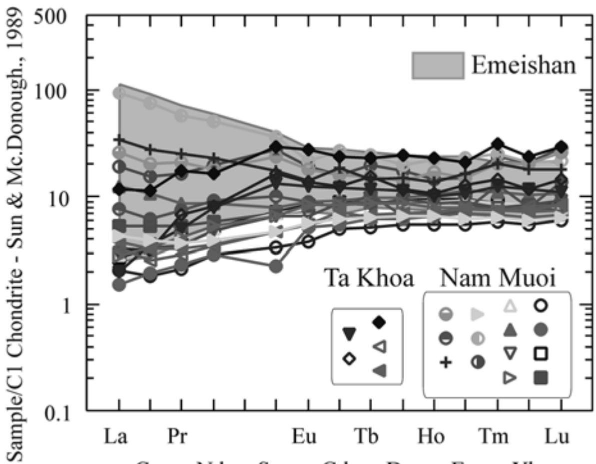

Fig. 2.3 Primitive mantle normalized patterns for Nam Muoi and Ta Khoa low-Ti magma series

ized for mantle plume-related magmas and melt inclusions in Iceland Hawaiian basalts (Sobolev et al. 2000; Breddam 2002). Basing on the REE contents and their distribution patterns (Table 2.5; Fig. 2.4) the komatiitic basalt associations may be divided into 4 groups: (1) peridotite, komatiite and komatiitic basalt group with a chondritic REE normalization pattern inclining to the left shows light-(L)REEs being up to 7 times higher, whereas, the heavy- (H)REEs being even higher, up to 9 times compared with the chondrite (Sun and McDonough 1989); (2) olivine basalts have REE contents 8–10 times higher than the given chondrite values, and show a

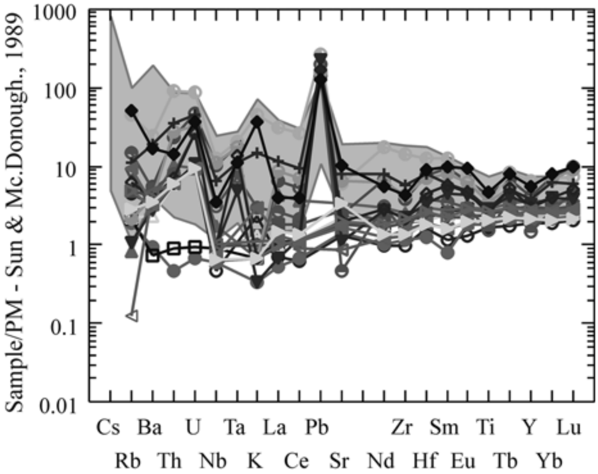

Fig. 2.4 Chondrite normalized patterns for Nam Muoi and TaKhoa low-Ti magma series

relatively flat normalizing curve; (3) Na-rich plagioclase basalt group has REE concentrations 20–40 times higher than the chondrite, showing Eu characteristically negative anomalies; (4) serpentinized peridotites of Ban Phuc massif as well as komatiitic pyroxenite in Nam Chim and Ban Mong dykes show clear differentiated rare earth element distribution, whose concentrations normally exceed those of the chondrite (e.g. Sun and McDonough 1989) 5–25 times with regard to LREEs and 3–9 times for HREEs. The Ban Phuc peridotite chondrite normalized distribution pattern is characterized by clearly Eu negative anomaly (Polyakov et al. 1996). This distribution feature may be related to secondary mineralization such that primary pyroxenes being replaced by serpentine, tremolite, chlorite as well as the appearance of biotite and magnetite. The $(Ce/Yb)_N$ ratios vary between 0.3 and 0.6 indicating a depleted mantle source. In addition, REE concentrations and Gd_N/Yb_N varying within 0.8–1.2 suggest a melting depth equivalent to spinel peridotite field. The olivine basalts show low Nb_N/La_N (0.31–0.42), falling in the field of oceanic island basalt (OIB) (Hanski et al. 2004). Similar geochemical features are also reported for Carboniferous picrites in the Shagin-Menglin ophiolite belt which were suggested to relate Paleotethyan oceanic plateau (Fang Nianqiao and Nin Gaoling 2003).

2.1.2.4 Re-Os and Sm-Nd Isotopic Compositions

14 whole rock Nam Muoi komatiitic samples were chosen for Re-Os and among these, 9 were chosen for Sm-Nd analysis. The samples being komatiite porphyry with olivine (samples G1448, G1456, 8/86, 11/86, 46/89, B6889, B6891, B6892) and needle-shaped clinopyroxene phenocrysts show MgO varying from 20.8 to 29.8 wt%. Other samples such as B6887, B6889 and B6865 were olivine cumulates having MgO between 22.6 and 30.9 wt% and showing such structural features to

Table 2.6 Representative Sm – Nd isotopic compositions of Nam Muoi komatiitic basalt associations (Hanski et al. 2004)

Sample ID	Rock type	Sm (ppm)	Nd (ppm)	$^{147}Sm/^{144}Nd$	$^{143}Nd/^{144}Nd$	ε_{Nd} (250)
B6887	Komatiite	0.6	1.48	0.2466	0.512957 ± 19	4.6
B6889	Komatiite	1.32	2.87	0.278	0.513184 ± 20	8
B6891	Komatiite	1.12	2.77	0.2446	0.513082 ± 10	7.1
B6892	Komatiite	1.2	2.65	0.274	0.513152 ± 10	7.5
G1456	Komatiite	1.13	2.45	0.2778	0.513112 ± 15	6.6
PI 1/86	Komatiite	0.7	1.8	0.2348	0.512869 ± 12	3.2
P9/86	Komatiite	0.8	1.97	0.2464	0.512883 ± 12	3.2
G1436	Ol-basalt	1.4	4.28	0.1972	0.512602 ± 30	−0.8
P73/89	Ol-basalt	2.95	13.06	0.1366	0.512158 ± 10	−7.5

suggest that their temperatures dropped slower while compared with other olivine-bearing porphyry magmas mentioned above. Sample 12/86 is komatiitic basalt (MgO =11.4 wt%); one of the other two samples has MgO lower than 10 wt% and spinifex texture for clinopyroxene, the other is a low-Ti basalt. Being sampled in a strongly metamorphosed zone (up to green schist facies) the collected samples were undeformed. The olivine-rich volcanic rocks are mostly well-reserved. Percentage of olivine being serpentinized and iddingsitized in 8/86 and 11/86 samples is about 50 % while in the other samples this secondary modification process occurs only about 25 % of the olivine grains. Cpx and Pl were not altered in most of the samples (Hanski et al. 2004).

Results of Sm-Nd and Re-Os isotopic compositions are shown in Table 2.6. Analytical procedure was described in detail in Hanski et al. (2004). Below are major comments from this report.

The initial $\varepsilon_{Nd(250)}$ data for komatiites and komatiitic basalts range from 3.2 to 8.0, whereas, for the low-Ti basalts the values are low, varying between −0.8 and −7.5. The high $\varepsilon_{Nd(250)}$ closer to 8 fall in the present depleted mantle field (DePaolo 1981; Goldstein et al. 1984). Correlation between the $\varepsilon_{Nd(250)}$ and the REEs is positive. Komatiites have the highest $^{147}Sm/^{144}Nd$ and the highest ε_{Nd}, the latter decreases as the corresponding $^{147}Sm/^{144}Nd$ decreases. This tendency explains basaltic lavas contaminated by high REE crust. Osmium contents are high in the komatiites, from 1.4 to 7 ppb, low in the komatiitic basalts, 1.2 ppb, and lowest in the basalts, at 0.12 ppb. There is apparent relationship between Os and MgO observed in the Song Da rift and Gorgona komatiites (Fig. 2.5). There is also close relationship between Os and Cr being observed in the Song Da rift volcanics except for Cr-spinel-bearing komatiitic basalts with almond-like structure. Rhenium contents in the Song Da rift volcanic magmas are low, from 0.07 to 0.96 ppb that show no clear relationship with MgO. Rhenium contents in the Song Da basalts are much lower compared with Gorgona basalt (1–3 ppb). In fact, Re contents in Song Da komatiites are also lower than those in Gorgona komatiites. Re and Cr in the two komatiite types do not show any clear relationship (Fig. 2.5). As a result of having high Os and low Re contents

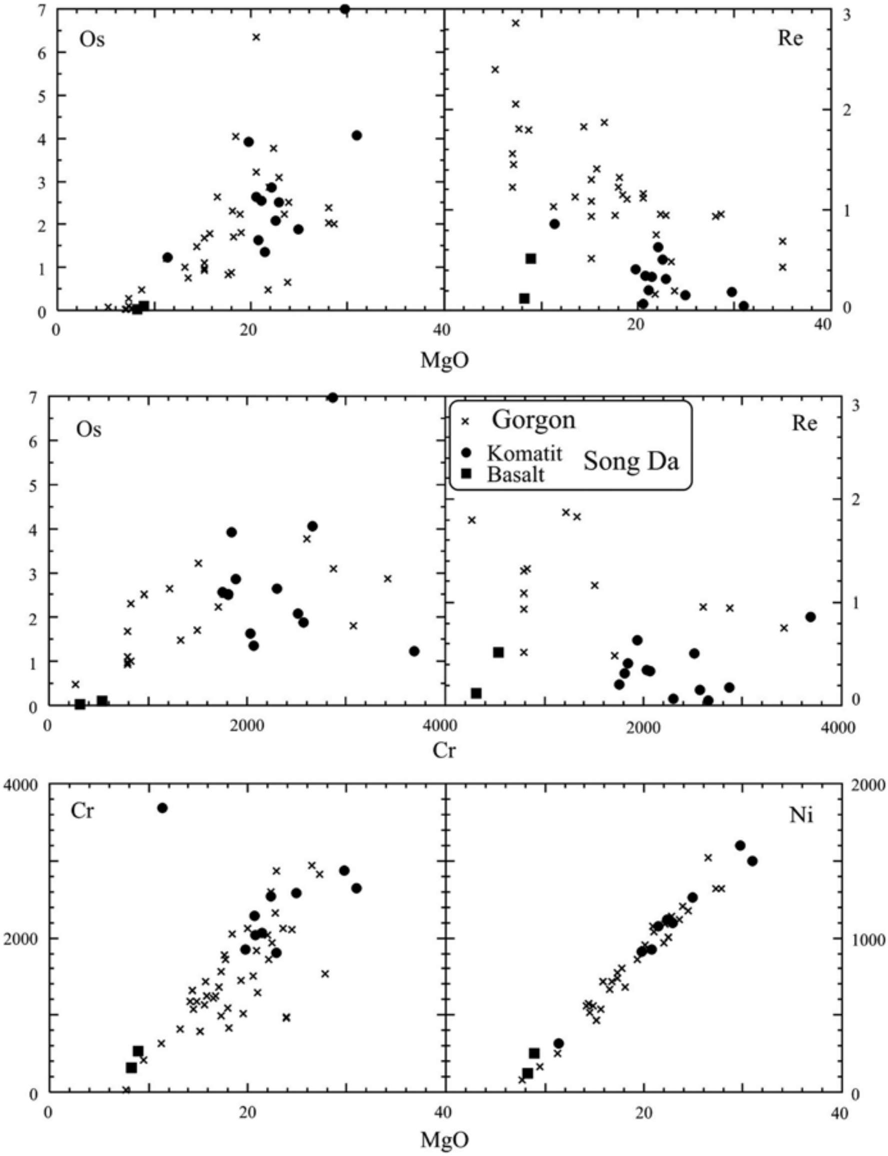

Fig. 2.5 Plots of Ni, Cr, Re and Os against MgO in Song Da rift komatiites (*circle*) and basalts (*square*) in comparison with Gorgona basalt – komatiite complex (*cross*) (The Song Da data are from Hanski et al. 2004)

^{187}Re/^{188}Os ratios in komatiites are low (<1.2 to 0.05; Table 2.7). Among the samples analyzed for Re-Os isotopes 12 samples formed an isochron that yielded an age of 270 ± 21 Ma and an initial ^{188}Os/^{187}Os = 0.12506 ± 0.00041 (γ_{Os} = +0.02 ± 0.4) (Fig. 2.5). Regardless of large uncertainty the age is consistent with previous Rb-Sr age at 257 ± 24 Ma (Hoa 1995; Polyakov et al. 1996), also consistent with age reported for basalts in the Emeishan large igneous province in China (Zhou et al. 2002).

Table 2.7 Representative of Re-Os isotopic compositions of Nam Muoi komatiitic basalt associations (Hanski et al. 2004)

Sample	Rock type	Re (ppb)	Os (ppb)	MgO (%)	$^{187}Os/^{188}Os$	$^{187}Re/^{188}Os$	Initial 7/8	γ0s
8/86	Komatiite	0.3168	2.511	22.13	0.12764	0.6078	0.12511	–0.2
11/86	Komatiite	0.18	6.995	29.76	0.12549	0.1239	0.12498	–0.3
9/86	Komatiite	0.1476	1.874	24.85	0.12769	0.3795	0.1261	0.6
B6865	Komatiite	0.5111	2.082	22.6	0.12995	1.1833	0.12501	–0.3
B6887	Komatiite	0.0421	4.075	30.94	0.12546	0.0498	0.12525	–0.1
B6892	Komatiite	0.4125	3.915	22.37	0.12752	0.5077	0.1254	0.1
B6889	Komatiite	0.6265	2.8413	22.08	0.1298	1.0627	0.12501	–0.1
B6891	Komatiite	0.2102	2.5286	21.05	0.12668	0.4004	0.12487	–0.3
G1456	Komatiite	0.3456	1.625	20.78	0.13005	1.0249	0.12577	0.4
46/89	Komatiite	0.3378	1.366	21.64	0.12962	1.192	0.12464	–0.5
G1448	Komatiite	0.0674	2.626	20.53	0.1255	0.1236	0.12498	–0.3
12/86	Komatiitic basalt	0.8586	1.238	11.39	0.14043	3.348	0.12645	0.9
G1436	Basalt	0.1188	0.0338	8.2	0.22075(7)	17.156	0.14914	19
	Basalt	0.0648	0.033	8.2	0.23833(7)	9.588	0.19831	58.2
P73/89	Basalt	0.5149	0.1166	8.93	0.26805	21.659	0.17765	41.8

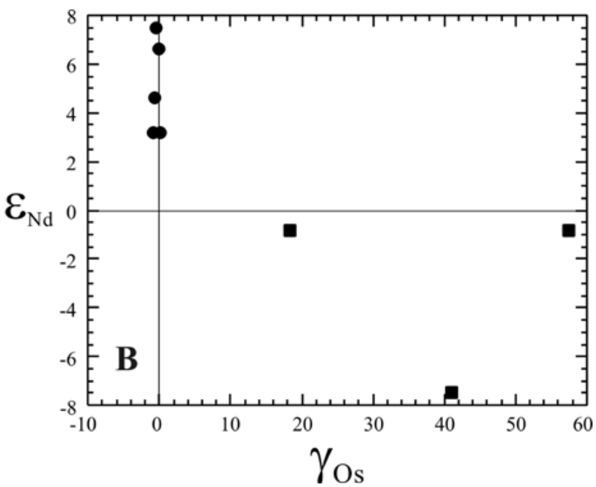

Fig. 2.6 Plots of 250 Ma initial γ_{Os} against ε_{Nd} for Song Da rift komatiites (*circle*) and basalt (*square*)

In contrast to the initial Nd isotopic ratios those vary widely from +3 to +8 the initial $^{187}Os/^{188}Os$ in komatiites change in a small interval from 0.1246 to 0.1264 (γ_{Os}=−5 – +0.9) and 0.1243 to 0.1260 (γ_{Os}=−0.7 – +0.6) (Table 2.7), calculated based on 250 Ma and 270 Ma, respectively. Two basaltic samples, G1436 and P73/89, show higher Os isotopic ratios compared with the initial γ_{Os} from +18 to +58. The initial γ_{Os} data in komatiites are nearly unchanged thus do not correlate with the correspondingly variable initial ε_{Nd} (Fig. 2.6). The basalts have higher γ_{Os} and lower ε_{Nd} compared with the komatiites.

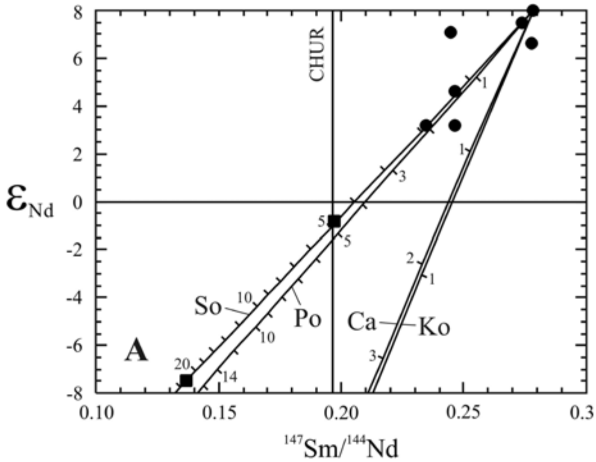

Fig. 2.7 Plots of $\varepsilon_{Nd(250Ma)}$ against $^{147}Sm/^{144}Nd$ for Song Da komatiites (*filled circle*) and basalts (*filled square*)

2.1.2.5 Isotopic Analytical Results

Geochemically Song Da rift komatiites are closely similar to Gorgona Cretaceous komatiites. Possibly they both were generated from long-term REE depleted mantle sources although the Gorgona komatiites show slightly higher ε_{Nd} (ca. +10) than Song Da rift komatiites (max. +8). Initial $^{87}Sr/^{86}Sr$ ratios of Song Da komatiites are 0.70348 (Hoa 1995; Polyakov et al. 1996) accompanied by high ε_{Nd} values, suggesting their being derived from a depleted mantle source. The strontium isotopic ratios are less radiogenic compared with those continental intraplate basalts, for example, the Siberian trap, while only slightly higher than those of Gorgona komatiites (at 0.7027, after Revillion et al. 2002). Majority of osmium isotopic ratios in komatiites from both Song Da and Gorgona are mostly similar to those reported for chondrite. As mentioned above, the geochemical similarity between Song Da and Gorgona komatiites suggests that their mantle sources may show many similar features in geochemistry and thermal state as well as melt generation (Herzberg and O'Hara 2002).

However, it is noteworthy that Song Da komatiitic basalt melts must have been through a continental crust having more heterogeneous compositions compared with the crust where Gorgona komatiitic melts having gone through. Song Da geochemically and isotopically enriched characters suggest the magmas may have been crustally contaminated. Plots of ε_{Nd} vs. $^{147}Sm/^{144}Nd$ show the komatiites lie between a depleted mantle and enriched Proterozoic and Archeanozoic sources suggesting a possible binary mixing (Fig. 2.7). For this mixing model, Archean basement may be Ca Vinh-type granito – gneiss (2800–2900 Ma) (Lan et al. 2001; Nam 2001), whereas gneiss of Song Chay formation and Po Sen-type calc-alkaline granite in northwestern Vietnam may serve as Proterozoic basement (Lan et al. 2000, 2001; Qui et al. 2000).

Proterozoic and Archean crustal contamination eventually leads to significantly decrease in ε_{Nd} and $^{147}Sm/^{144}Nd$, even at as a small percentage as 1–2 % involvement of crustal material. Isotopic results of the Song Da pluton- volcanic associations are not ready to tell what their true, uncontaminated mantle source was; for REE budgets in komatiitic magmas are sensitive to crustal input, therefore, the last eruptive Song Da komatiites may represent their true mantle source most similar to that of Gorgona source (for example, having $\varepsilon_{Nd}=+10$). If this is true the uncontaminated mantle of Song Da depleted komatiites may have $^{147}Sm/^{144}Nd$ ratios about 0.315 and their LREE concentrations may have been even smaller than the acquired results. Basalts in the komatiite – basalt associations having low $\varepsilon_{Nd,}$ high γ_{Os}, low Nb and Ta, aside from undergoing fractional crystallization and melt differentiation, may have been contaminated by crustal material as much higher percentage as 5–20 %. However, in contrast to Sm – Nd isotopic systematics, Re-Os system in komatiites is not affected by a small input of continental crust material, this possibly because Os concentration is very high in komatiites (>1 ppb) compared with that in continental crust (ca. 0.05 ppb) (Walker and Nisbet 2002). Therefore, osmium isotopic ratios possibly reflect the true mantle source signature even there is evidence of crustal involvement. Notice that as because Os content in komatiitic basalts is much smaller (ca. 0.03 ppb) than in komatiites, they, therefore, may be affected by crustal contamination more than the latter; as a result their primary osmium isotopic ratios may be higher.

Mixing model using initial isotopic compositions of komatiitic magmas and basement rocks represented by Ca Vinh (Ca) Archean granite in northwestern Vietnam and Conglin (Ko) granite in southwest China is illustrated in Fig. 2.7. Mesoproterozoic basement is represented by Song Hong (So) and Po Sen (Po) complexes (Lan et al. 2000, 2001; Qui et al. 2000). Values participating in the mixing model include $\varepsilon_{Nd(250)}$, Sm, Nd, respectively, for komatiite: +8, 1 ppm, 2.2 ppm; Ca: −33.4, 13.6 ppm, 78.7 ppm; Ko: −44.9, 3.02 ppm, 27.6 ppm; So: −10.3, 7.5 ppm, 41.1 ppm, Po: −131.1, 5.2 ppm, 32.9 ppm.

Apparently, the Nd and Os isotopic compositions of Song Da rift and Gorgona komatiite – basalt indicate that mantle sources of these two Phanerozoic komatiitic series were most similar to the presently defined depleted MORB mantle (DMM). Recent studies have shown that komatiitic magma can be produced by highly depleted mantle such as DMM under hydrous pressure. Based on experimental and geochemical data Grove et al. (1999) and Parman et al. (2001) suggested that Barberton 3.49 Ma komatiites were generated by hydrous melting of peridotite at a subduction zone. They observed that geochemical features of Barberton komatiitic basalt are mostly similar to boninites produced by melting of depleted peridotites which experienced previous melting events at an Archean mid-ocean ridge or a back-arc spreading axis. Shimizu et al. (2001) suggested that late Archean Belingwe komatiite was produced by mantle plume melting containing about 0.5 % water evidenced by high water contents in melt inclusions in Cr-spinel. Experimental studies of high pressure melting with or without water showed that anhydrous melting of mantle plume may also be a potential generation of komatiites (Asahara and Ohtani 2001).

Anhydrous melting of a DMM source may be considered as melting temperature for komatiitic generation in the upper mantle is rather low relative to that required for an anhydrous melting. High MgO in komatiites have been produced by anhydrous melting at melting temperatures that are 140–320 °C higher than a MORB melt (Herzberg and O'Hara 2002). This thermal state is difficult to present in the depleted upper mantle condition (Arndt and Christensen 1992). Hydrous melting mechanisms may be best explanation for Song Da rift komatiites for there are expressions of crustal contamination being explained by the input of highly incompatible elements from subducted lithospheric slab into the komatiite upper mantle source. Although Song Da komatiites can be produced by H_2O-saturated DMM source; but this is less likely for the LREE depletion nature of the komatiites. Mantle plume-related magmas, for example, OIB types, are more hydrous compared with MORB. The OIB magmas are thought not only being produced by hotspots but also by 'wet'-spot (Shilling et al. 1980; Wallace 1998; Nichols et al. 2002). Water contents in plume-related magmas depend on the magmatic composition; the more enriched in incompatible elements is the richer water magma (Danyushevsky et al. 2000). It has been explained that during OIB magma melting and crystallization water behaves as a lithophile element whose incompatibility may be comparable to that of La or Ce (Michael 1995). Melt inclusions in underwater volcanic rocks and in primary minerals from arc magmas show a positive correlation between H_2O/Y and Ce_N/Yb_N (r =0.99) (after Danyushevsky et al. 2000; Dixon and Clague 2001; Saal et al. 2002). If geochemical behavior of water in Song Da komatiitic melts was as mobile as any incompatible element most of their depleted primary magmas with Ce_N/Yb_N around 0.3 must have H_2O/Y lower than 200; meaning that the water concentration was no more than 0.03 wt%. Because there is no other evidence on the relationship between water and LREE in non-arc basaltic magmas, it may suggest that highly depleted Song Da komatiites may be produced by anhydrous melting of a primarily depleted mantle source. However, it is noteworthy that if Rb, Ba and Sr enrichment was inherited from their respective mantle source this phenomenon has to be expressed by slight increase in H_2O/Ce ratio and high water content in their mantle source.

Sub-continental lithosphere mantle (SCLM) can be source mantle for komatiites; however, like the DMM, thermal factor required for melting is not adequate. Although some komatiites may be produced in SCLM by metasomatism (Walker and Stone 2001); however, this possibility is ignored for the osmium isotopic data do not provide such evidence.

In the recent years there have been opinions that some mantle plume show geochemically and isotopically depleted characters therefore depleted mantle, not necessary DMM, can play a major component in a mantle plume source (Hart et al. 1992; Arndt et al. 1997; Fitton et al. 1997). However, the nature of depleted mantle and its role in a (mantle) plume are subject for wide debates (Kerr et al. 1995). Depleted mantle plume and DMM occur in Iceland where plume overlies Atlantic mid-ocean ridge. Highly variable geochemical and isotopic characteristics in Iceland and Reykenes basalts may be viewed as consequences of mixing between DMM and enriched Iceland mantle plume (Sun et al. 1975). However, based on geochemical and isotopic (especially Pb) properties of the Iceland basalts several researchers stated that basalts and picrites that were depleted in incompatible elements may be produced by mantle other than DMM (Kerr et al. 1995; Kempton et al. 2000; Chauvel and Hémond 2000). Using Nb/Y vs. Zr/Y correlation diagram (Fitton et al. 1997) Iceland depleted magma is different from N-MORB. This opinion has not been shared by many. For example, Hanan et al. (2000) suggested that geochemical variations in Iceland and Reykjanes basalts and picrites may reflect mixtures of enriched mantle plume and surrounding mantle similar to N-MORB.

Determination of mantle sources for continental flood basalts (CFB) is even more difficult given the fact that if the magmas were produced by sub-lithospheric source, this may be obscured either by crustal assimilation or interaction with SCLM. In reality, geochemical and isotopic N-MORB-like magmas are rare in CFB (Thomson et al. 1983; Carlson 1991). The most depleted magmas are commonly observed for highly primitive lavas, for example, picrite from North Atlantic magmatic province (Saunders et al. 1997) and Horing Bay dykes in Namibian coastal areas (Thomson and Gibson 2000), and perhaps these Song Da rift komatiites.

Addition of a small amount of crustal material does not affect the Os isotopic compositions in komatiites; therefore, Os isotope can be the most important signature of the mantle source. Komatiites are the major component of Gorgona magma, their chondritic Os isotope composition plots in DMM field, mixture of peridotite, MORB glass and ophiolitic chromite (Walker et al. 2002). This combination is not compatible with any theoretically known average DMM. Whereas, Song Da komatiites show twice lower radiogenic values compared with a DMM at 250 Ma, whose radioactive evolution is estimated based on an average composition of chromite of ultramafic magmas in a Phanerozoic ophiolitite formation (Walker et al. 2002).

If mantle source for the Song Da komatiites is not DMM their chondritic Os component may be residual portions of oceanic lithosphere having depletion history closely similar to that of DMM. Kerr et al. (1995) presented that ultramafic lava in Caribbean large igneous province may be formed by depleted sources introduced from lower mantle. They argued that highly refractory (and depleted) oceanic lithosphere subducted to core mantle boundary was later brought up by a plume.

Therefore, geochemical and isotopic features of the Song Da high-Mg, low-Ti magmas suggest that they may be closely associated with mantle plumes which originated from the core mantle boundary. This southeast Asian magmatic province is not the only example, Permian – Triassic Siberian trap may also be another plume-related. Given the fact that Norinsk-type Ni-Cu-PGE mineralization is well developed in the Siberian trap; naturally, this potential resource can also be discovered in the Song Da rift region.

2.1.2.6 Composition of Primitive Melts and T-P Parameters

Experiments show that low-Al komatiite partial melts are formed under hydrous condition at depths between 500 and 650 km, while high-Al komatiites are formed by higher melting degrees, at depths lower than 450 km (Ohtani et al. 1989). Other

Table 2.8 Chemical compositions (wt%) of primitive melts for Nam Muoi and Ta Khoa komatiitic basalt associations

No	1	2	3	4	No	1	2	3	4
SiO_2	46.99	44.17	47.48	46.21	Na_2O	1.08	0.32	1.17	0.86
TiO_2	0.61	0.56	0.92	0.70	K_2O	0.11	0.11	0.57	0.26
Al_2O_3	11.54	10.36	11.09	11.00	P_2O_5	0.10	0.08	0.10	0.09
FeO	11.37	12.28	11.59	11.75	P_1	0.0	0.0	0.0	0.0
MgO	17.58	23.24	17.03	19.28	P_2	25	50	22	30
CaO	10.62	8.88	10.05	9.85	T°C	1510	1660	1500	1560

Remark: P_1, P_2 are crystallizing (P_1) and melting (P_2) pressures. T°C: melting temperature. 4 is average of 1, 2, and 3

experiments (e.g. Ryabchikov and Bogachikov 1984) showed that Iilgar-type primitive komatiitic melt was produced by 50 % partial melting of primitive mantle lherzolite at P=35–37 kb and T=1775–1825 °C. According to these authors Barberton-type komatiitic melt may be produced by 60–65 % partial melting of lhezolite at higher pressure and temperature, ca. 50 kb and 1875–1975 °C, respectively. They suggested that the difference between picrite – basalt and komatiite – basalt rock types depends on the variation and nature of fluids; komatiite – basalt melts are associated with 'dry' fluids while picrite – basalt and picrite – dolerite melts being produced under hydrous condition. Our recent studies may be used to expand the latter explanation. Our results showed that komatiite – basalt, in comparison to picrite – basalt and picrite – dolerite associations, are more enriched in Al, Mg, Ca, Ni, Co, Cr, Yb and Lu, while they are poorer in Ti, Fe, P, Rb, Sr, V, Nb, Ta, Zr and REEs (Balykin and Petrova 2000). Besides, we have found that evolution trend from Precambrian komatiitic basalt associations to Phanerozoic komatiitic basalt and picritic basalt associations is expressed by gradual decrease in of normative hypersthene (Balykin 2004). Primitive composition extrapolation of low-Ti ultramafic – mafic rocks shows result that is correspondent to komatiitic basalt (Table 2.8).

Calculation of normative co-existing minerals for the komatiitic basalt association shows a high pressure assemblage of Ol-Px-Gr while the total of accessory minerals such as apatite, ilmenite and phlogopite does not exceed 1–2 %, the latter amount is about 5–7 % in picritic basalt and dolerite associations. This may mean that the mantle source for picritic basalt associations is more enriched in incompatible elements and fluids compared with that of the komatiitic basalt. The above explanation is in favor to a suggestion that komatiitic melt is produced by progressive melting of a depleted mantle source, which had undergone previous melting to produce basaltic melt enriched in incompatible elements (Arndt 1976). Plots of Song Da high- and low-Ti magmas on a Fo-Di-Py diagram (Davies and Schairer 1965) show that the primitive komatiitic basalt melt is closely similar to observed komatiitic basalt, whereas the primitive melt of picritic basalt and dolerite is similar to that of melanobasalt (Balykin et al. 2001; Balykin 2004).

Modeling crystallization of primitive melts of komatiite, komatiitic basalt, olivine basalt was conducted using software program 'Comagmat-3.3' (Ariskin et al.

1993). This program allows for selecting initial melt compositions (among the given hypothetical melts) which provide co-existing mineral assemblages that are best fit for both calculated (normative composition) and real mineral assemblages as well as their crystallizing order. Comagmat 3.3 program can determine liquidus temperatures with accuracy within ±10 °C of more than 70 % of mineral cases; while accuracy of phase compositions is within ±2 % (for plagioclase us ±2.8 %).

In general, the composition of Song Da komatiitic basalt initial melt is MgO = 17.0–23.2 wt%. High aluminum content in clinopyroxene indicates that the initial crystallization pressure of Ol and Cpx was not lower than 10 kb (Balykin et al. 2001).

2.1.2.7 General Remark on the Komatiitic Basalt Associations

The Song Da komatiite – basalt associations in northwestern Vietnam may be viewed as part of Emeishan large igneous province, formed by melting of the top of a mantle plume under the Yangtzi craton during Permian – Triassic time (Chung et al. 1998). Following India- Eurasian collision during the Pliocene – Miocene (ca. 27–22 Ma) left lateral movement to the northeast of Ailao Shan – Red River shear zone displaced the now Song Da rift magmatic associations from the main basaltic province in southwest China. The komatiitic basalt associations currently are distributed within the axial area of the rift zone, comprising lava flows, dykes as well as lenses of pluton-volcanic mafic rocks. Komatiites intercalated with komatiitic basalts are dominant in the lower section, while upper sections are comprised by komatiitic basalt, olivine basalt being overlain by plagiobasalt. Eruption ages of the magmas are 257 ± 24 Ma (by Rb/Sr age dating), and 270 ± 21 Ma (by Re/Os age dating). The magmas, varying from high-Al komatiites to low-Al basalts, are characterized by having low alkalis, very low titanium and high Mg. They are rich in Ni, Co, Cr, Cu and poor in Fe, Rb, Ba, Sr, Nb, Ta, Nd, Hf, Zr and REEs. The komatiites and komatiitic basalts are relatively low in REE concentrations; however, their LREE contents are 2–7 times higher, and HREE are 5–9 times higher than those of the chondrite. Song Da rift komatiitic basalt associations are rare phenomena for Phanerozoic komatiitic basalt activity, not to mention the presence of Ni-Cu and PGE ore-formation is believed to associate with the komatiites. Digital modeling showed that the initial melt composition was correspondent to komatiitic basalt.

Song Da komatiites show many geochemical indexes similar to Gorgona Island's Cretaceous komatiites. They both are high-Al (compared with Archean komatiites), low incompatible elements and low LREE/HREE ratios. In difference from Gorgona komatiitic melts formed as part of oceanic magmatic plateau of Caribbean type, Song Da magmas were mantle derived interacted with continental lithosphere. This is evidenced by the presence of Proterozoic sialic signature in Nd isotopic systematics and LILE concentrations in high-Mg Song Da magmas; while their accompanying Os isotopes show signatures which are closer to a DMM source. Moreover, initial isotopic features and depletion of incompatible elements (e.g., Ce/Sm $\leq$0.3) of the Song Da komatiitic basalt magmas are closely similar to chondrite values.

This may mean that, the Song Da source had been depleted in incompatible and light rare earth elements for long period while showing Re/Os isotopic ratios similar to that of chondrite. In summary, Song Da komatiites may serve as a rare example of continental plateau basalts which contain geochemical and isotopic signatures of their primary source mantle.

Systematic variation of water and incompatible elements in present oceanic island basalts is not related to a subduction zone, therefore, we may assume that Song Da primitive komatiitic melts being depleted in water and incompatible elements were generated at the anhydrous topmost part of a mantle plume. High Mg in their primary melts indicate deep rooted origin and that melting temperature was about 200 °C higher than average potential temperature of a MORB primary source (Herzberg and O'Hara 2002). This unusual high temperature can only be expected at the hottest center of an initial plume. Geochemical and isotopic properties of the Song Da magmas and those from Caribbean oceanic plateau and North Atlantic large igneous provinces provide more evidence to support that plume-related melts may be formed at the boundary between lower mantle and core.

2.1.3 High-Ti Basalt Associations

2.1.3.1 Spatial Distribution and Geology

As mentioned above, high-Ti mafic volcanic and accompanying sub-volcanic magmas belong to three association-types: andesite – basalt (with rhyolite), picrite – basalt and trachyandesite-trachydacite – trachybasalt. They are widely distributed in marginal areas of the Song Da structure. Andesite – basalt associations outcrop mainly in the Cam Thuy and Son La Pass areas, southwestern wing of the structure (Fig. 2.1). Picrite – andesite – basalt associations have only been discovered in Nam So, northeastern tip of Song Da structure; while rhyolite – basalt associations are popular in Kim Boi, Vien Nam (Doi Bu), Ba Vi and Van Yen – Phu Yen (Suoi Chat). Trachyandesite – trachydacite – trachybasalt associations have only been found in the Nam Muoi area, northwestern side of Song Da structure. Outcrops of felsic rocks of various sizes and chemical compositions are being found in each high-Ti basalt field. Felsic magmas are rarely encountered among andesite – basalt and picrite – andesite – basalt associations, but highly common among rhyolite – basalt and trachyandesite-trachydacite – trachybasalt formations. Felsic volcanic and sub-volcanic rocks associated with rhyolite – basalt rock type show calc-alkaline geochemical character; while those found in trachyandesite – trachydacite – trachybasalt associations are sub-alkaline type.

Basalts and andesitobasalts in the Cam Thuy area are characterized by aphanitic sometimes doleritic texture, almond-shaped structure; albitization, actinolitization and chloritization (greenization), previously termed as spilite, are strongly developed. Basalts in the Kim Boi, Ba Vi (Vien Nam – Doi Bu), Phu Yen – Van Yen (Suoi Chat) show similar petrologic characteristics.

High-Ti basalts (andesite – basalt association) in the Son La Pass area are geochemically homogenous, showing aphanitic texture, almond-shaped structure filled with chlorite, epidot, albite and chalcedony. The basaltic groundmass is microdiabas, pilotaxitic texture with main microlites being uralitized plagioclase and clinnopyroxene. No olivine is being observed in andesite – basalt associations, but fine-grained, diffused titanomagnetite is common. In many geological cross-sections aside from basalts encountered also are andesitobasalt and andesite. Among the basalt, andesitobasalt and andesite outcrops found also are small sub-volcanic bodies or dykes of diabase or gabbro-diabase.

Basaltoids belonged to the picrite – andesite – basalt associations in northwestern margin of the Song Da structure form an elongate belt running in the northwest – southeast direction from upstream of Nam So, south of boundary between China and Vietnam, in the north. A full cross-section for this association can be observed in an area northwest of Tam Duong town, Lai Chau province. Major constituents of the cross-section are mafic volcanic magmas, including picritodolerite (melanobasalt), dolerite, basalt and andesitobasalt (leucobasalt); picrite and andesite types are minor. Picrite is found in picritodolerite and other mafic volcanic cross-sections in the Nam So upstream area. The magma is fine-grained aphanitic texture and dark colored. Among the major rock-forming minerals are Cpx microlites in the groundmass, serpentinized or talcized olivine phenocrysts and altered plagioclase. Titanomagnetite is widely found. Picrite is chemically sub-alkaline and picritobasalt (ankaramite), having high Mg, low Al but high potassic alkalinity. The magma is also relatively high in Ti and P oxides. Picrite having high Mg and Ti contents has so far been found in the Nam So area. This picrite type is chemically different from ultramafic magmas in picrite – diabase association outcropped in the Ba Vi area although the picrite shows closely spatial connection with high-Ti volcanic magmas in this area (Polyakov et al. 1996). Chemically ultramafic magmas in the picrite – dolerite association are low-Ti and relatively low-alkaline type.

Picritodolerites (melanobasalt) are wider spread compared with picrites, and show spatial relation to basalts and andesitobasalts. The magmas are dark-colored, aphyric or porphyritic texture with Cpx and Pl in the phenocryst; the groundmass is ophitic, microdoleritic or taxitic. They are high in Mg and Ti, relatively high in alkalis, including K. Chemically they are close to sub-alkaline picritobasalt although their MgO contents are slightly lower.

Sub-alkaline basalts and andesitobasalts (leucobasalts) are dominant in Nam So and Phong Tho cross-sections. Chemical compositions of the leucobasalts are high variable; among these porphyritic basalts are most common with Cpx and Pl being in the phenocryst. The minerals present at various proportions forming different rock types such as pyroxene basalt or plagio-basalt. The groundmass is hialopilitic or microdoleritic. Almond-shaped structure is sometimes occurred where almonds are filled with epidote and calcite. The basalt and andesitobasalt rock types show relatively high T, K and P oxides. Besides, andesitodacites are also found but at a minor scale. Found also are sub-volcanic bodies comprised of diabase and dolerite.

Structurally volcanic cross-sections in the areas of Cam Thuy, Bac Yen – Van Yen (Suoi Chat), Hoa Binh, Kim Boi – Ba Vi, Vien Nam (Doi Bu) show distinct features compared with those in the Son La Pass, Nam So and Nam Muoi areas. Firstly, commonly found are high-Ti and alkaline basalts equivalent to trachybasalt (Na-type), sub-alkaline felsic, and (Na-rich) alkaline magma types. Secondly, bright-colored lava flows and dyke-bodies are spread in, respectively, Kim Boi and Vien Nam – Bac Yen. Chemically the basalts are similar to basalts in andesite – basalt association in the Cam Thuy area (described above), in that they are high in TiO_2, relatively high Na_2O and P_2O_5. Small lherzolite, pyroxenite intrusive bodies and diabase dykes are commonly discovered in Ba Vi within the Song Da structure, Chim Thuong in southern margin of the Tu Le basin, and Dong Nghe – Suoi Can – Nga Hai belonging to the Phan Si Pan uplift and neighboring areas. At an outcrop in the Chim Thuong area there are a number of small-sized intrusive bodies comprising a chemically complex rock types including picrite and diabase, where picrite being distributed at the center and diabase being located at the periphery. These bodies normally cut conformably Paleozoic sediment-metamorphic (including shale, quartzite) strata. Other small intrusive bodies of peridotite (and picrite) are observed in the Ba Vi area, these bodies show closely spatial relationship with the above high-Ti mafic volcanic magmas and were previously grouped to Ta Khoa ultramafic magmas as Ban Xang complex (Tran Van Tri and Truong Cam Bao 1977). These Ba Vi and Dong Nghe – Suoi Can ultramafic bodies together with high-Ti diabase dykes were later grouped as picrite-diabase and viewed as sub-volcanic formations in affiliated with trachyandesite – trachydacite – trachbasalt associations in the Ba Vi area (Polykov, Yem et al. 1996). These are also high-Ti (relatively to low-Ti ultramafic volcanics), Mg, low- Al and relatively low alkalis. Phenocryst minerals include Ti-augite and kaersutite. The diabase is high-Ti and sub-alkaline (Na-K alkaline).

The intrusive ultramafic magmas are Pl-bearing wehrlite and lherzolite with a minor amount of clinopyroxenite, tremolitite, serpentinite and asbestos lenses. Main rock-forming minerals are Ol ($f_{Ol} = 14.1–16.5$), Cpx and small amount of highly basic Pl. Accessory minerals include of biotite, Cr-spinel and magnetite. In some intrusive olivine gabbro, gabbro-norite and gabbro are also found.

It is noteworthy that a meimechite (high magnesian alkaline) variation was found in the Hoa Binh hydropower dam area. Based on petrologic and chemical compositions this magma is equivalent to volcanic picrite. This picrite rock type was also found in the Doi Bu area but was described as olivine basalt (Lu 2004). Details of the magma so far have not yet been studied; but there is possibility that the magma is volcanic counterpart of intrusive peridotite being commonly observed in the Ba Vi area. Typical volcanic picrite is porphyritic with phenocryst of variously serpentinized olivine and pyroxene, and glassy groundmass.

2.1.3.2 Mineralogical and Geochemical Characteristics

Chemical compositions of major rock-forming minerals and ores of the studied pluton – volcanic series are shown in Tables 2.9, 2.10, 2.11, and 2.12. The olivines are highly magnesian, equivalent to forsterite – chrysolite. Olivines in mafic rocks are high ferrous (up to 22.5 %). The clinopyroxenes are low-Ti and alkaline, although

Table 2.9 Chemical compositions (wt%) of olivines in mafic-ultramafic intrusives, Dong Nghe – Suoi Can area (Polyakov et al. 1996)

Sample ID	FeO	MgO	CaO	NiO	Ni. ppm	f_{Ol}
Picrite. lherzolite and wehrlite						
B6185	16.01	43.6	0.3	0.09	707	17.1
B6187	17.75	41.53	0.24	0.08	644	19.3
B6809	14.59	44.08	0.33	0.27	2130	15.7
G1414	9.19	48.55	0.25	0.39	3074	9.6
G1415	10.35	47.91	0.15	0.36	2812	10.8
G1417	8.55	48.97	0.24	0.37	2907	8.9
G1418	12.51	45.55	0.29	0.26	2028	13.4
Clinopyroxenite and melagabbro-dolerite						
G1419	14.9	43.69	0.3	0.29	2278	16.1
G1420	20.49	39.37	0.27	0.24	1893	22.5

Table 2.10 Chemical compositions of clinopyroxenes in high-Ti mafic volcanic in Song Da structure (EPMA analyzed at IGM, SB-RAS)

Sample ID	T1552	H608	P-9	H616	H614	B6816
	Nam So area					
SiO_2	51.34	49.74	50.63	51.72	50.49	49.31
TiO_2	0.57	0.95	0.92	0.85	1.1	1.64
Al_2O_3	3.26	5.42	3.12	1.9	2.75	2.6
Cr_2O_3	0.58	1	0.1	0.81	0.01	0.02
FeO	4.73	5.2	7.58	6.52	11.13	10.56
MgO	16.08	14.48	14.9	17.1	15.76	14.48
CaO	21.49	22.2	21.17	19.49	17.08	20.78
Na_2O	0.28	0.44	0.44	0.38	0.39	0.36
f_{Cpx}	15.6	16.8	22.2	17.7	29.9	29
Wo	44.8	47.9	44.3	40.4	34.4	42.2
En	46.6	43.3	43.4	49.2	46	41
Fs	8.6	6.9	12.3	10.4	19.6	16.8

Sample ID	H669	47/88	52/88	51/88	57/88	G1414	P156	P163	G1405
	Vien Nam area					Suoi Can area			
SiO_2	47.73	51.75	50.69	50.06	52.91	52.19	50.12	50.19	52.02
TiO_2	2.45	0.46	0.91	1.46	0.34	0.46	1.38	0.75	0.75
Al_2O_3	4.4	2.72	1.8	2.99	1.29	3.03	3.82	4.22	2.46
Cr_2O_3	–	1.13	–	0.09	0.57	0.63	0.17	0.99	0.01
FeO	10.37	3.82	13.14	10.13	5.21	6.88	6.77	5.12	10.16
MgO	13.24	17.08	14.27	14.65	18.52	18.02	15.42	15.86	16.31
CaO	19.95	22.06	17.75	19.31	20.12	18.11	20.9	21.69	17.26
Na_2O	0.72	0.27	0.37	0.4	0.16	0.26	0.38	0.24	0.19
f_{Cpx}	30.5	11.2	34.1	28	13.7	17.6	19.7	15.7	25.9
Wo	42.9	45.2	37.1	40.5	40.3	37.3	45.6	45.2	36
En	39.7	48.7	41.5	42.8	51.6	51.7	46.8	46.2	47.4
Fs	17.4	6.1	21.4	16.7	8.1	11	7.6	8.6	16.6

Table 2.11 Chemical compositions of plagioclases in high-Ti mafic volcanics in Song Da structure (Polyakov et al. 1996)

Sample ID	SiO_2	Al_2O_3	FeO	CaO	Na_2O	K_2O	An	Ab	Or
Nam So area									
H608	54.71	27.68	0.14	9.49	5.91	0.28	48	51	1
P-9	61.75	21.11	0.73	3.97	7.88	3.91	20	60	20
Son La area									
B6816	52.95	27.94	0.97	11.78	4.8	0.4	58.6	39	2.4
T1687	58.65	21.63	3.42	10.13	5.69	0.05	50	50	
H668	54.63	28.06	0.34	9.69	5.73	0.16	49	50.5	0.5
H675	56.99	26.75	0.34	8.54	7.04	0.09	40	60	-
H676	52.83	23.17	2.99	10.46	6.95	0.09	51	49	-

Table 2.12 Chemical compositions of Cr-spinel in high-Ti lherzolite in Song Da structure (Polyakov et al. 1996)

Sample ID	TiO_2	Al_2O_3	Cr_2O_3	Fe_2O_3	FeO	MgO	MnO	NiO	ZnO
	Đồng Nghê – Suồi Cẩn area								
G1417	0.33	16.22	48.93	4.34	18.42	10.19	0.54	0.1	0.06
G1418	0.29	16.64	48.37	4.56	18.08	10.42	0.53	0.16	0.03
T509	0.39	15.78	49.39	4.43	17.31	10.85	0.53	0.12	0.07
P156	0.33	17.42	49.37	4.03	14.82	12.76	0.48	0.1	0.05
T510	0.27	15.3	49.2	5.15	19.98	9.16	0.56	0.1	0.05

some are high-Ti and –Na. Chemical compositions of ore minerals such as Cr-spinel and sub-Fe-Cr-picotite are nearly invariable. Detailed descriptions are given in (Hoa 1995; Polyakov et al. 1996).

Representative chemical compositions of the sub-volcanic pluton and volcanic rocks are given in Tables 2.13 and 2.14. Plots of TiO_2 vs. SiO_2 and P_2O_5 vs. SiO_2 (Fig. 2.8) of Song Da samples in comparison with Emeishan representatives suggest the following.

Except for metabasalts from Cam Thuy, Hoa Binh, Vien Nam, Suoi Chat and picrite from Nam So, the samples are high in Ti and K that vary in large intervals (TiO_2 = 2.1–3.5 wt%; K_2O = 1.1–1.8 wt%). Their P_2O_5 contents are also high that vary between 0.2 and 0.55 wt%. These geochemical features are closely similar to those of Emeishan, East African rift and Oslo Paleo-rift. Dark-colored picrite, picritobasalt (pircritodolerite) in the Nam So area also show Ti, Mg and alkaline geochemical similarity to Emeishan picrite and picritobasalt.

Judging the behavior of major elements, especially characteristic elements such as Ti, K and P, Song Da high-Ti ultramafic – mafic magmas are comparable with corresponding magmatic types in large igneous provinces (LIP) such as Emeishan. Plots of MgO vs. TiO_2, Na_2O and K_2O among the Song Da magmatic associations show that Ti, Na and K increase from andesite – basalt (Cam Thuy and Son La areas) to picrite – andesitobasalt – basalt and trachyandesite – trachydacite – trachybasalt

Table 2.13 Major (%wt) and trace element (ppm) compositions in high-Ti basalts in the Nam Muoi area (1–4: analyzed in Finland; 5–7: analyzed at IGM, SB-RAS)

	IGCP-11	IGCP-12/1	IGCP-7/2	IGCP-8	16/86	P141/89	P142/89
Sample ID	1	2	3	4	5	6	7
SiO_2	47.6	47.4	48.2	50.2	50.33	47.85	48.52
TiO_2	2.14	3.51	3.54	4.26	4.04	2.64	2.56
Al_2O_3	13.9	11.6	13.9	13.4	13.18	15.03	12.97
Fe_2O_3	13.32	14.4	13.93	15.09	13.85	11.4	12.66
MnO	0.2	0.14	0.19	0.08	0.18	0.16	0.2
MgO	5.57	5.31	5.66	4.48	3.49	6.04	6.96
CaO	8.23	3.65	5.66	3.91	6.74	8.96	6.7
Na_2O	4.34	3.66	2.8	5.72	2.77	3.25	2.14
K_2O	0.61	0.73	1.62	1.56	3.24	1.07	1.09
P_2O_5	0.23	0.55	0.6	0.65	0.58	0.37	0.35
V	352	407	386	390			
Cr	170	29	40	6			
Ni	78	46	57	38			
Cu	222	188	490	193			
Zn	117	130	154	86			
Ga	20	27	33	29			
Sr	400	281	408	79			
Zr	151	263	395	424			
Ba	305	101	467	200			
Ce	45	73.7	115	153	112.2	52.3	40.4
Dy	5.68	7.98	6.91	7.87			
Er	3.18	4.73	3.73	3.91			
Eu	1.75	3.78	3.03	3.17	3.9	2.5	2.1
Gd	5.92	11.1	10.5	12	11.6	8.9	5.6
Ho	1.12	1.51	1.33	1.38			
La	20.1	32.2	51.1	68.2	59.3	24.8	19.1
Lu	0.29	0.84	0.46	0.26	0.4	0.4	0.3
Nd	23.6	46	57.3	66.3	58.3	30.6	23.8
Pr	5.39	9.97	14	17.5			
Sm	5.09	12.8	11.2	11.5	14.3	8.2	6.4
Tb	0.99	1.67	1.41	1.61	1.7	1.4	0.9
Tm	0.41	1.09	0.54	0.4			
Yb	2.62	4.54	3.03	2.63	3.4	2.9	2.3
Sc	44	25.6	20.9	25.2			
Y	33.4	34.9	36.7	42.3			
U	0.71	1.71	2.09	1.71			
Th	3.22	4.19	8.1	8.47			
Hf	4.01	6.59	7.87	8.82			
Nb	15	27.7	41	53.2			
Rb	18.2	29.6	27.7	24.8			
Ta	0.88	2.14	2.15	3.31			

Table 2.14 Major (%wt) and trace element (ppm) compositions of high-Ti picrite and basalt in the Nam So (1–5) and Son La (7–8) areas

	H615	H617	P18	T1495	T1648	H639	B6816	B6817
Sample ID	1	2	3	4	5	6	7	8
SiO_2	46.07	50.09	43.89	44.99	48.47	46.27	46.31	48.47
TiO_2	2.35	2.69	2.14	4.44	1.58	2.31	3.38	3.41
Al_2O_3	14.02	11.36	6.55	13.10	14.64	9.04	14.09	13.60
Fe_2O_3	13.87	12.34	12.76	15.64	13.93	13.23	14.12	13.37
FeO	0.00	0.00	0.00	0.00	0.00	0.00	0.00	0.00
MnO	0.24	0.18	0.19	0.24	0.23	0.22	0.23	0.25
MgO	7.32	7.72	22.91	4.67	7.40	12.16	5.06	4.61
CaO	8.24	8.85	10.22	9.98	10.31	12.78	10.55	8.80
Na_2O	3.29	3.06	0.21	2.26	2.39	2.49	2.98	3.29
K_2O	1.25	0.82	0.17	1.16	0.79	0.63	1.03	1.81
P_2O_5	0.20	0.30	0.27	0.56	0.18	0.25	0.60	0.72
Ce	43	64	49	113	29	68	58.90	78.50
Eu	1.80	2.30	1.70	3.30	1.39	2.20	2.90	3.40
Gd	4.90	6.60	4.50	9.30	5	5.40	8.70	11.60
La	20.40	31.30	23.60	56.20	13.60	33.00	27.40	37.80
Lu	0.20	0.30	0.20	0.50	0.45	0.20	0.30	0.40
Nd	24	34	26	55	17	36	35.20	45.20
Sm	5.60	7.80	5.60	11.70	4.50	7.40	9.60	12.00
Tb	0.80	1.00	0.70	1.50	0.85	0.80	1.30	1.70
Yb	1.80	2.20	1.20	3.30	3	1.70	2.30	2.30

H615 – H617: dolerite; P19: picrite; T1495: basalt; H639: picritodolerite; B6816-6817: basalt (Hoa 1995; Polyakov et al. 1996)

(Tables 2.13 and 2.14; Fig. 2.8). Note that K_2O/Na_2O ratios in Vien Nam – Doi Bu and Suoi Chat dacites and rhyodacites are usually <1; whereas the ratios are >1 in trachyandesite-trachydacite in the Nam Muoi area. Regardless of having difference K/Na ratios all the felsic magmas show high Nb (74–126 ppm), Ta (5–9 ppm), La (71–140 ppm), Ce (135–259 ppm). Primitive mantle normalized trace element distribution patterns for alkaline felsic magmas are intraplate in character (Fig. 2.9).

According to the chemical compositions picrite-diabase sub-volcanic – volcanic associations may be divided into three groups: ultramafic (plagioperidotite, olivine plagiopyroxenite); sub-ultramafic (dark-colored pyro-xenite) and mafic (gabbro and diabase). The pyroxenite, gabbro and diabase being usually high in Ti, relatively high alkalis, especially K, are viewed as typical high-Ti mafic magmas. The wehrlite and lherzolite are low in Ti and alkalis, in general, but relatively high when compared with ultramafic magmas in komatiite – basalt associations having the same MgO concentrations mentioned earlier. Cu, Ni, Co and Cr are relatively low in the basaltoids (including picrite and picritodolerite), lower compared with mafic magmas in the komatiite – basalt associations; whereas these elements are high in lherzolite and wehrlite in the Ba Vi and Nam Chim areas. The enrichment is similarly observed in Permian mafic magma in the Cao Bang area, northeast Vietnam (see below).

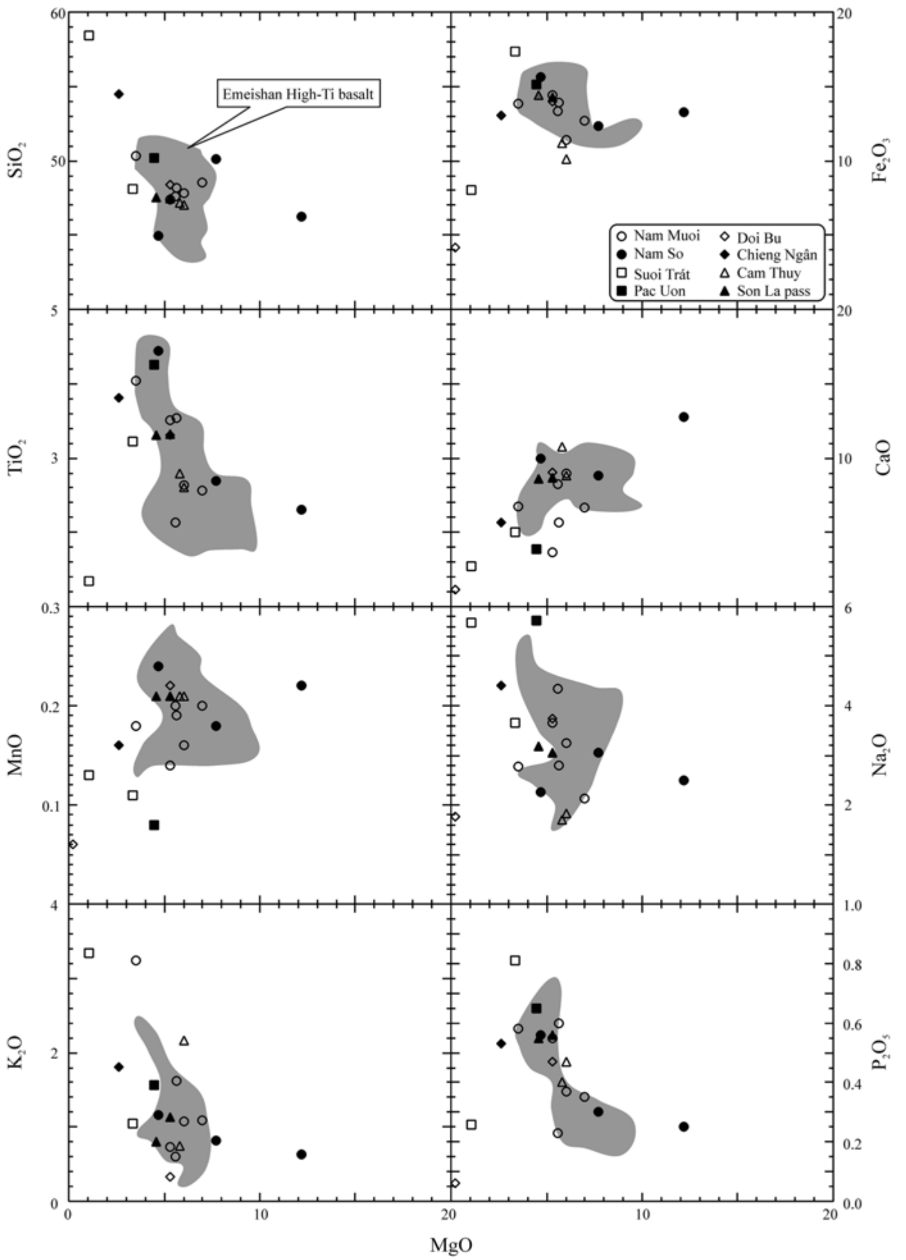

Fig. 2.8 Harker diagram for Song Da high-Ti basaltoids in comparison to high-Ti Emeishan (China) basalts

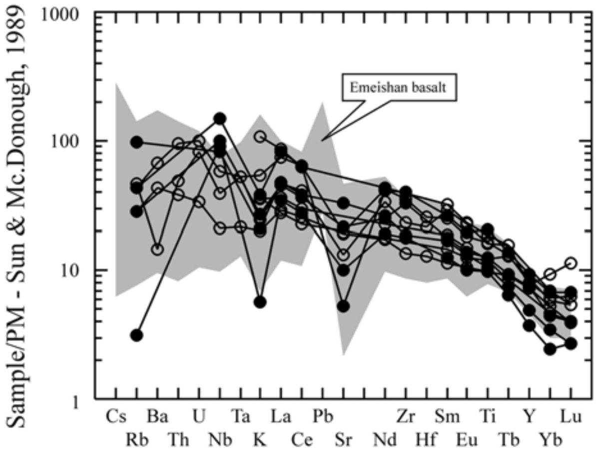

Fig. 2.9 Primitive mantle normalized trace element distribution patterns of Song Da Nam Muoi and Nam So high-Ti volcanics (Emeishan data are from Chung et al. (1998))

Song Da Permian basaltoids in the Nam So and Nam Muoi areas are high in Nb (26–53 ppm), Zr (151–424 ppm) and the rare earths, especially LREE (Tables 2.13 and 2.14). Primitive mantle normalized distribution patterns reveal positive anomalies at Nb, Ta, Rb, Zr, Ce and Th, while some samples show slightly negative anomalies at Nb and Zr, and strongly negative anomaly at Sr (Fig. 2.9); these are typical geochemical features of sub-alkaline continental rift-related basaltoids. Enrichment of Nb, Th, Zr and LREE is clearly observed in trachybasalt, trachyandesite and trachydacite in the Nam Muoi area where some sub-alkaline felsic magmas show high enrichment is Nb (97–164 ppm), Ta (6 ppm) and Zr (622–896 ppm) (Polykov et al. 1996). Primitive mantle normalized patterns of the trachyandesite and trachydacite magmas (Figs. 2.9 and 2.10) are intraplate in nature, mostly similar to Permian – Triassic trachyte and trachyrhyolite magmas in the nearby Tu Le structure. Absolute values of (for example) Nb and Zr in the basalts and bright-colored volcanic rocks are usually 20–100 (for Nb) or 10–40 times higher compared with given primitive mantle values (e.g. Sun and McDonough 1989). Dark-colored picrites and picritedolerites in the Nam So area are also characterized by high Nb, Ta, Th, Ce and Zr; these features distinguish the magmas from lhezolites in the picrite-diabase associations. In classification plots of Zr/Y vs. Zr most of the high-Ti Song Da basaltoids fall in field of intraplate magmatism (Hoa et al. 1998; Hoa 2002).

Basalt and trachybasalt in the Suoi Chat, Van Yen, Vien Nam, Kim Boi and Doi Bu areas show oceanic island basalt-like primitive mantle normalized distribution patterns similar to that observed for basalt and picritobasalt in the Nam So and Nam Muoi areas, in that they both are enriched in Rb, Nb, Ta and the rare earths (Figs. 2.11 and 2.12). Having different in K/Na ratios the felsic magmas of magma associations in these areas show high Nb (74–126 ppm), Ta (5–9 ppm), La (71–140 ppm), and Ce (135–259 ppm). Primitive mantle normalized distribution patterns of

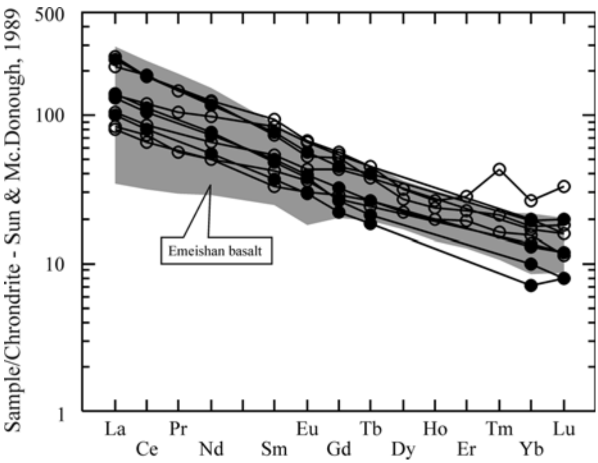

Fig. 2.10 Primitive mantle normalized trace element distribution patterns of Song Da high-Ti basalts in the Nam Muoi and Nam So areas (Emeishan basalts are after (Chung et al. 1998))

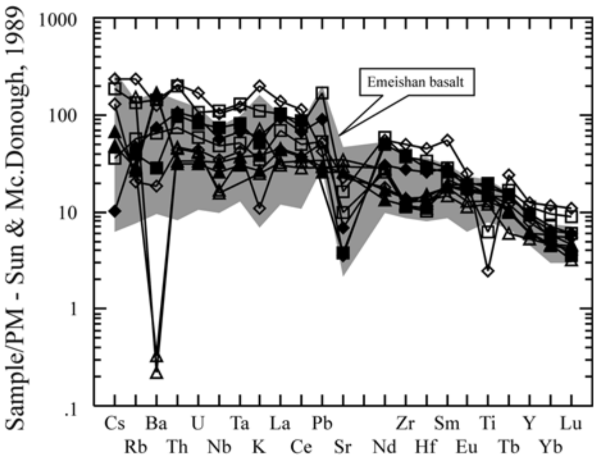

Fig. 2.11 Primitive mantle normalized trace element distribution patterns of Song Da high-Ti basalts in the Cam Thuy, Vien Nam, Suoi Chat and Doi Bu areas (Emeishan basalts are after (Chung et al. 1998))

the alkaline felsic volcanics are typical intraplate (Fig. 2.11). Note that lherzolite in the Thu Cuc area are low in Rb (3.99–4.77 ppm), Sr (40.88–57.97 ppm), Zr (20.49–25.69 ppm), Nb (1.76–2.26 ppm) and the rare earth elements (Table 2.15). Except for having slightly higher LREE, these geochemical compositions are mostly similar to low-Ti ultramafic magmas (komatiites) (Fig. 2.13). Gabbro associated with high-Ti basalts in the Suoi Chat area is characteristically high Rb (31.4 ppm), Sr (437.9 ppm), Zr (57.49 ppm), Nb (18.01 ppm) and the rare earths, similar to those in high-Ti basalts in the area (Figs. 2.11, 2.12).

Table 2.15 Geochemical compositions of lherzolite and picrite in the Ba Vi and Thu Cuc areas

Sample ID	10-123	10-124	10-126	IGCP-47	IGCP-48		IGCP-47	IGCP-48
SiO_2	42.5	42.1	39.3	44.46	41.67	Zr	25.69	20.49
TiO_2	0.73	0.81	0.66	0.52	0.41	Nb	2.26	1.76
Al_2O_3	5.4	6.4	5.8	8.59	5.9	Ba	33.12	26.27
Fe_2O_3*	10.46	9.32	10.57	11.45	11.55	La	2.25	1.81
MnO	0.11	0.12	0.13	0.17	0.17	Ce	4.91	3.82
MgO	25.97	25.58	27.37	23.09	28.52	Pr	0.67	0.53
CaO	5.44	5.41	4.18	8.44	6.3	Nd	2.26	1.76
Na_2O	0.09	0.13	0.07	0.49	0.02	Sm	1.03	0.79
K_2O	0.05	0.05	0.13	0.08	0.05	Eu	0.35	0.27
P_2O_5	0.11	0.1	0.07	0.03	0.02	Gd	1.28	0.97
Mkn	8.2	8.57	10.65			Tb	0.26	0.19
Total	99.7	99.35	99.68			Dy	1.72	1.37
Cu	24	32	4			Ho	0.39	0.29
Ni	1493	1415	1336	934.4	1250	Er	1.13	0.87
Co	85	86	83			Tm	0.17	0.12
V	190	196	78	191.9	150.8	Yb	1.12	0.87
Cr	2390	2388	2941	2417	3176	Lu	0.17	0.13
Sc				30.72	24.23	Hf	0.69	0.55
Cs				0.3	0.15	Ta	0.15	0.12
Rb				4.77	3.4	Pb	0.47	0.1
Sr				57.97	40.48	Th	0.52	0.45
Y				10.85	8.25	U	0.12	0.11

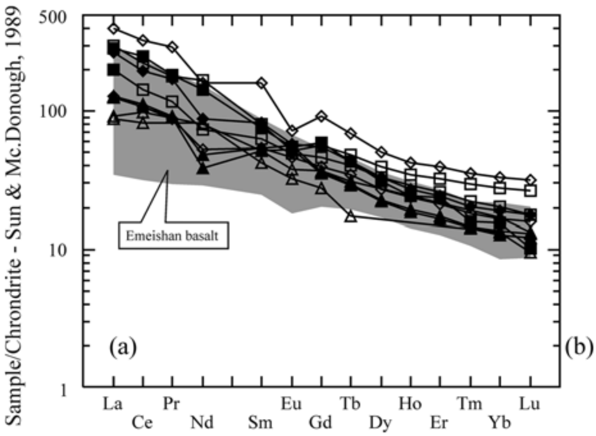

Fig. 2.12 Primitive mantle normalized trace element distribution patterns of Song Da high-Ti volcanics in the Cam Thuy, Vien Nam, Suoi Chat and Doi Bu areas (Emeishan data are after (Chung et al. 1998))

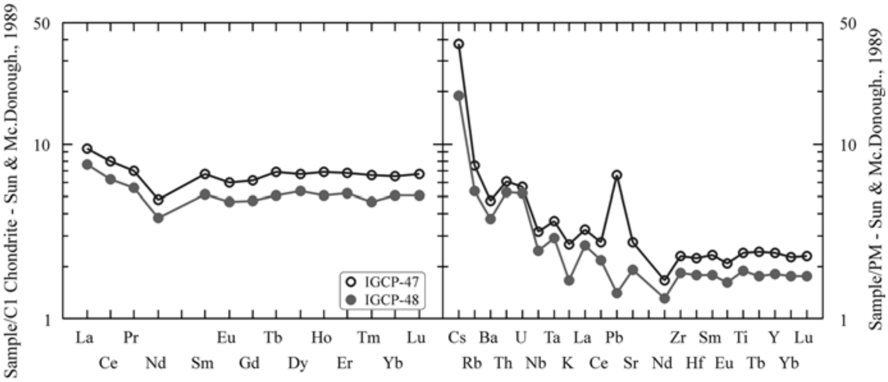

Fig. 2.13 Chondrite and primitive mantle normalized rare earth and trace element distribution patterns of Ba Vi lherzolites (Sun and McDonough 1989)

Initial $^{87}Sr/^{86}Sr$, $^{143}Nd/^{144}Nd$ and $^{206}Pb/^{204}Pb$ isotopic ratios of high-Ti basalts, rhyodacite in the Doi Bu and Suoi Chat areas vary, respectively, between 0.706–0.709, 0.5119–0.5124, and 18.32–23.5, indicating involvement of crustal material in the magma source (Hoang et al. 2004). Crustal involvement in the Song Da magma source or during magmatic melt evolution may be possible for the northwestern rim of the Song Da rift is bordered by the Truong Son mountain range where marginal pluton-volcanic magmas are wide-spread.

2.1.3.3 Source and Melt Generation Characteristics

The geochemical and isotopic compositions of Song Da mafic and ultramafic volcanic rocks indicate that their mantle source or magmatic melts were contaminated by crustal materials. However, questions remained are whether crustal involvement happened in the source mantle or after melt generation, e.g. wall-rock assimilation. Assuming dacite (and trachydacite) and rhyolite (trachyrhyolite) being formed by fractional crystallization of basaltic melts generated in the lithospheric mantle, therefore involvement of any crustal material must be related to previously subducted slab into the mantle. The difference in elemental enrichment of Nb, Ta, Zr and other incompatible elements in the high-Ti volcanic magmas, as well as geochemical signatures of sub-oceanic lithospheric mantle in the low-Ti magmas may be explained by specific Song Da rift magmatic evolution in the Permian and lithospheric mantle source heterogeneity under South China craton's marginal continents. Besides, the formation of (high field strength elements: HFSE) Nb-, Ta-, Zr-rich trachybasalts and their fractional sub-alkaline felsic magmas in the Nam Muoi, Suoi Chat and Doi Bu areas may be explained by low-degree partial melting of sources having been depleted by previous melting events to form high-Ti magmatic melts in the Cam Thuy, Son La and Nam So areas (Polyakov et al. 1996).

However, this model is lacking of formation order of basaltic melts in northwestern and southeastern Song Da rift. Up to date, there only a few relative reliable age data have been reported including 257 ± 24 Ma for komatiitic basalt in the axial area of Song Da rift (Hoa 1995; Polyakov et al. 1996) and 270 ± 21 Ma (Hanski et al. 2004); whereas Carboniferous (283 ± 21 Ma) (Hoang et al. 2004) may need additional evidence. It is interesting that Rb/Sr age dating on dacite whole rocks believed to genetically related to Song Da basalts yielded a Permian – Triassic age of 256 ± 15 Ma (e.g. Hoang et al. 2004).

The above description of regional geochemical features of Song Da high-Ti basaltic associations suggests that mantle sources from where high-Ti melts being generated may be locally 'independent' present. There was also possibility that during the HFSE-rich magma generation additional alkaline and incompatible elements having been introduced by a mantle plume. This remark is supported by (Anh et al. 2011) showing that the high-Ti basalts have relatively restricted ranges of $(^{87}Sr/^{86}Sr)_i$ (0.7048–0.7079) and εNd(t) values (−5.7 to +3.1) indicating weak lithospheric signature that may be related to their trace element-rich nature and this is consistent with abundant earlier studies suggesting that the high-Ti basalts at Song Da or elsewhere in the ELIP formed from low degrees of partial melting (Xu et al. 2001; Wang et al. 2007). The silisic rocks (trachyandesite, trachydacite) which occur in high-Ti basalts of the Song Da structure having εNd(t) values from −0.1 to 0.6, was formed by fractional crystallization of the associated high-Ti basalts.

References

Ariskin AA, Frenkel MY, Barmina GS, Nielsen RL (1993) COMAGMAT: a Fortran program to model magma differentiation processer. Comput Geosci 19:1155–1170

Arndt NT (1976) Melting relations of ultramafic lavas (komatiites) at 1 atm and high pressure. Carnegie Inst Wash Yearb 75:551–561

Arndt NT, Christensen U (1992) The role of lithospheric mantle in continental flood volcanism; thermal and geochemical constraints. J Geophys Res 97(10):967–10981

Arndt NT, Kerr AC, Tarney J (1997) Dynamic melting in plume heads; the formation of Gorgona komatiites and basalts. Earth Planet Sci Lett 146:289–301

Asahara Y, Ohtani E (2001) Melting relations of the hydrous primitive mantle in the CMAS-H2O system at high pressures and temperatures, and implications for generation of komatiites. Phys Earth Planet Inter 125:31–44

Balykin PA (2004) Composition and PT-conditions of melting of parental magmas for komatiite-basalt, picrite-basalt, and picrite-dolerite complexes. 32nd IGC, Florence

Balykin PA, Petrova TE (2000) Petrological types and genesis of komatiite-basalt, picrite-basalt and picrite-dolerites complexes. Russ Geol Geophys 41:1098–1111

Balykin PA, Polyakov GV, Petrova TE, Shelepaev PA, Tran Trong Hoa, Ngo Thi Phuong, Hoang Huu Thanh (2001) Composition of initial melts for Permo-Triassic and Triassic-Jurassic ultramafic-mafic complexes in North Vietnam. Rep RAS 378(2):225–229 (in Russian)

Breddam K (2002) Kistufell: primitive melt from the Iceland mantle plume. J Petrol 43:345–373

Bùi Minh Tâm, Tô Văn Thụ (1995) New report on volcanic and dyke phased magmas in the Phong Tho (Lai Chau) area. Geology – mineral resources and oil and gas of Viet Nam I, pp 89–96 (in Vietnamese with English abstract)

Carlson RW (1991) Physical and chemical evidence on the cause and source characteristics of flood basalt volcanism. Aust J Earth Sci 38:525–544

Chauvel C, Hémond C (2000) Melting of a complete section of recycled oceanic crust: trace element and Pb isotopic evidence from Iceland. Geochem Geophys Geosyst 1, 1999GC000002

Chung SL, Jahn BM, Genyao W, Lo CH, Bolin C (1998) The Emeishan flood basalt in SW China: a mantle plume initiation model and its connection with continental breakup and mass extinction at the Permian-Triassic boundary. In: Flower MFJ, Chung SL, Lo CH, Lee TY (eds) Mantle dynamics and plate tectonics in East Asia, vol 27, AGU geodynamics series. American Geophysical Union, Washington, DC, pp 47–58

Danyushevsky LV, Eggins SM, Falloon TJ, Christie DM (2000) H_2O abundance in depleted to moderately enriched mid-ocean ridge magmas; part I: incompatible behaviour. Implications for mantle storage and origin of regional variations. J Petrol 41:1329–1364

Davies BTC, Schairer JF (1965) Melting relations in the join diopside-forsterite-pyrope at 40 kilobars and at one atmosphere. Carnegie Inst Wash Yearb 64:123–126

De Paolo DJ (1981) Neodymium isotopes in the Colorado Front Range and crust – mantle evolution in the Proterozoic. Nature 291:684–687

Dixon JE, Clague D (2001) Volatiles in basaltic glasses from Loihi Seamount, Hawaii: evidence for a relatively dry plume component. J Petrol 42:627–654

Do Dinh Toat (1987) Petrology of Upper Permian and Upper Permian – Lower Triassic effusives in Cam Thuy – Ba Vi area. PhD dissertation, Hanoi University of Geology and Mining

Dobresov NL (2005) The Asian's large igneous provinces (250Ma): Siberian's and Emeishan's traps (plateau-basalts) and associated granitoids. Geol Geophys 46(9):870–890

Fang Nianqiao, Nin Gaoling (2003) Late paleozoic ultramafic lavas in Yunnan, SW China. J Petrol 44(1):141–157

Fitton JG, Saunders AD, Norry MJ, Hardarson BS, Taylor RN (1997) Thermal and chemical structure of the Icelandic plume. Earth Planet Sci Lett 153:197–208

Gatinsky YG (1986) Geodymanics of Southeast Asia in relation to the evolution of ocean basins. Palaeogeogr Palaeoclimatol Palaeoecol 55:127–44

Gatinsky YG, Thuc DD (1982) Geological structure and development of the Song Da peleorift zone in Vietnam. Bull Mineral Soc (Vietnam) 57:12–25

Goldstein SL, O'nions RK, Halmington PJ (1984) A Sm-Nd isotopic study of atmospheric dusts and particulates from major rive systems. Earth Planet Sci Lett 70:221–236

Grove TL, Parman SW, Dann JC (1999) Conditions of magma generation for Archean komatiites from the Barberton Mountainland, South Africa. In: Fei Y, Bertka CM, Mysen BO (eds) Mantle petrology: field observations and high pressure experimentation: a tribute to Francis R. (Joe) Boyd, vol 6, The geochemical society, special publication. Geochemical Society, Houston, pp 155–167

Hanan BB, Blichert-Toft J, Kingsley R, Schilling JG (2000) Depleted Iceland mantle plume geochemical signature: artifact of multicomponent mixing? Geochem Geophy Geosyst 1, 1999GC000009

Hanski E, Walker RJ, Hubma H, Polyakov GV, Balykin PA, Tran Trong Hoa, Ngo Thi Phuong (2004) Origin of the Permian-Triassic komatiites Northwestern Vietnam. Contrib Miner Petrol 147:453–469

Hart SR, Hauri EH, Oschmann LA, Whitehead JA (1992) Mantle plumes and entrainment; isotopic evidence. Science 256:517–520

Herzberg C, O'Hara MJ (2002) Plume – associated ultramafic magmas of Phanerozoic age. J Petrol 43:1857–1883

Izokh AE, Polyakov GV, Tran Trong Hoa, Balykin PA, Ngo Thi Phuong (2005) Permian-Triassic ultramafic-mafic magmatism of Northern Vietnam and Southern China as expression of plume magmatism. Russ Geol Geophys 46(9):942–951

Kempton PD, Fitton JG, Saunders AD, Nowell GM, Taylor RN, Hardarson BS, Pearson G (2000) The Iceland plume in space and time: a Sr-Nd-Pb-Hf study of the North Atlantic rifted margin. Earth Planet Sci Lett 177:255–271

Kerr AC, Saunders AD, Tarney J, Berry NH, Hards VL (1995) Depleted mantle-plume geochemical signatures: no paradox for plume theories. Geology 23:843–946

Khain VE, Balukhovsky AN (1993) Geotectonic. Mesozoi and Cenozoic. AVIAR, 451 p

Lan CY, Chung S-L, Jason Jiun-San Shen, Lo CH, Wang PL, Tran Trong Hoa, Hoang Huu Thanh, Mertzman SA (2000) Geochemical and Sr-Nd isotopic characteristics of granitic rocks from Northern Vietnam. J Asia Earth Sci 18:267–280

Lan CY, Chung SL, Lo cH, Lee TY, Wang PL, Li H, Dinh Van Toan (2001) First evidence for Archean continental crust in Northern Vietnam and its implications for crustal and tectonic evolution in Southeast Asia. Geology 29(3):219–222

Metcalfe I (1996) Pre-Cretaceous evolution of SE Asian terranes. In: Hall R, Blundell D (eds) Tectonic evolution of Southeast Asia. Geological Society Special Publications 106, London, pp 97–122

Michael P (1995) Regionally distinctive sources of depleted MORB: evidence from trace elements and H_2O. Earth Planet Sci Lett 131:301–320

Ngo Thi Phuong (1994) Permo-Triassic high-Magnesium volcano-plutonic associations in the Song Da structure. PhD dissertation. Thesis, Institute of Geology and Mineralogy, SB RAS, Novosibirsk, 24 pp

Ngo Thi Phuong, Tran Trong Hoa, Tran Tuan Anh (2001) Petro-minerallogical characteristics of the P2-T1 basalts-komatiite association in the Ta Khoa Anticline, Song Da Zone (NW Vietnam. J Geol Ser B, No 17–18, pp 10–19

Nguyen Dac Lu (2004) The relationship between volcanic rocks of Da River and Viet Nam areas and copper-gold mineralization. North Vietnam Geol Mapp Div, Geol Miner of Vietnam 4:166–174 (in Vietnamese)

Nguyen Hoang, Nguyen Đac Lu, Nguyen Van Can (2004) Paleozoic volcanics in the Song Da structure: Rb-Sr age of Doi Bu volcanics. J Geol A281:11–17 (in Vietnamese with English abstract)

Nichols ARL, Carroll MR, Höskuldsson A (2002) Is the Iceland hot spot also wet? Evidence from the water contents of undegassed submarine and subglacial pillow basalts. Earth Planet Sci Lett 202:77–87

Ohtani E, Kawabe I, Moriyama J, Nagata Y (1989) Partitioning of elements between majorite garnet and melt and implication for petrogenesis of komatiite. Contrib Mineral Petrol 103:263–269

Parman SW, Grove TL, Dann JC (2001) The production of Barberton komatiites in an Archean subduction zone. J Geophys Res Lett 28:2513–2516

Polyakov GV, Balykin PA, Glotov AI et al (1991) High-magnesian volcanites in Da river zone. In: Proceedings of the second conference on geology of Indochina, HN, 11–13 Nov 1991, vol 1, pp 247–261

Polyakov GV, Nguyen Trong Yem, Balykin PA, Tran Trong Hoa, Hoang Huu Thanh, Tran Quoc Hung, Ngo Thi Phuong, Petrova TE, Van Van V (1996) Permian – Triassic mafic and ultramafic formations in northern Viet Nam. Science and Technology Publ, Hanoi, 172 p (in Vietnamese)

Qiu YM, Gao S, McNaughton NJ, Groves DI, Ling W (2000) First evidence of >3.2 Ga continental crust in the Yangtze craton of South China and its implications for Archean crustal evolution and Phanerozoic tectonics. Geology 28:11–14

Révillon S, Chauvel C, Arndt NT, Pik R, Martineau F, Fourcade S, Marty B (2002) Heterogeneity of the Caribbean plateau mantle source: Sr, O and He isotopic compositions of olivine and clinopyroxene from Gorgona Island. Earth Planet Sci Lett 205:91–106

Ryabchikov ID, Bogachikov OA (1984) Physico-chemical conditions of formation and differentiation of Karelsk's komatiites. Geochemistry, No 5, pp 625–638 (in Russian)

Saal AE, Hauri EH, Langmuir CH, Perfit MR (2002) Vapour undersaturation in primitive mid-ocean-ridge basalt and the volatile content of Earth's upper mantle. Nature 419:451–455

Saunders AD, Fitton JG, Kerr AC, Norry MJ, Kent RW (1997) The North Atlantic igneous province. In: Mahoney JJ, Coffin MF (eds) Large igneous provinces: continental, oceanic and planetary flood volcanism. American Geophysical Union, Washington, DC, pp 45–93

Schilling J-G, Bergeron MB, Evans R (1980) Halogens in the mantle beneath the North Atlantic. Phil Trans Roy Soc Lond A297:147–178

Shimizu K, Komiya T, Hirose K, Shimizu N, Maruyama S (2001) Cr-spinel, an excellent micro-container for retaining primitive melts – implications for a hydrous plume origin for komatiites. Earth Planet Sci Lett 189:177–188

Sobolev AV, Hofmann AW, Nikogosian IK (2000) Recycled oceanic crust observed in ‘ghost plagioclase’ within the source of Mauna Loa lavas. Nature 404:986–990

Sun SF, McDonough WF (1989) Chemical and isotopic systematics of oceanic basalts: implication for mantle composition and processes. In: Saunders AD, Norry NJ (eds) Magmatism in ocean basins. Geol. Soc. Spec Pub 42, London, pp 313–345

Sun SS, Tatsumoto M, Schilling JG (1975) Mantle plume mixing along the Reykjanes Ridge axis; lead isotopic evidence. Science 190:143–147

Thompson RN, Gibson SA (2000) Transient high temperatures in mantle plume heads inferred from magnesian olivines in phanerozoic picrites. Nature 407:502–506

Thompson RN, Morrison MA, Dickin AP, Hendry GL (1983) Continental flood basalts … arachnids rule OK? In: Hawkesworth CJ, Norry MJ (eds) Continental basalts and mantle xenoliths. Shiva, Nantwich, Cambridge, MA, pp 158–185

Tong Dzuy Thanh, Vu Khuc (eds) (2005) Stratigraphic divisions of Vietnam. National University Publ, Hanoi, 504 p (in Vietnamese)

Tran Ngoc Nam (2001) SHRIMP U-Pb isotopic age dating on zircons of the Ca Vinh and Xom Giau complexes. J Geol A262:1–11 (in Vietnamese with English abstract)

Tran Trong Hoa (ed) (1995) Study of Mesozoic – Cenozoic magmatism and its mineralization potential. Final report for national project KT- 01–04 (1992–1995). Archives of the National Center for Science and Technology Information, Hanoi (in Vietnamese)

Tran Trong Hoa (2002) Subdivision and correlation of Permian – Triassic basaltoid associations in the Song Da structure (NW Vietnam). Geol Ser B 19–20:22–30

Tran Trong Hoa (ed) (2005) Intraplate magmatism in Viet Nam and related mineral resources. Final report for Viet Nam – Russian collaboration protocol (2002–2004). Archives of the National Center for Science and Technology Information, Hanoi, 333 p (in Vietnamese)

Tran Trong Hoa (2007) Intraplate magmatism in North Vietnam and related metallogeny. Dissertation of Dr. of Science. Institute of Geology and Mineralogy, Siberian Branch, RAS, Novosibirsk, 382 p

Tran Trong Hoa, Hoang Huu Thanh, Tran Tuan Anh, Ngo Thi Phuong, Hoanh Viet Hang (1998a) High – Ti Permian-Triassic basaltoid of Song Da rift. Material composition and geodynamic forming conditions. J Geol Ser A 244:7–15

Tran Trong Hoa, Hoang Huu Thanh, Tran Tuan Anh, Ngo Thi Phuong, Hoang Viet Hang (1998b) High-Ti basaltoidic formations in the Song Da rift zone: chemical compositions and geodynamic conditions of magma genesis. J Geol A244:7–15 (in Vietnamese with English abstract)

Tran Trong Hoa, Tran Tuan Anh, Ngo Thi Phuong, Pham Thi Dung, Tran Viet Anh, Izokh AE, Borisenko AS, Lan CY, Chung SL, Lo CH (2008) Permo-Triassic intermediate-felsic magmatism of the Truong Son belt, eastern margin of Indochina. Compt Rendus Geosci 340:112–126

Tran Trong Hoa, Tran Tuan Anh, Pham Thi Dung, Lan Ching-Ying, Usuki Tadashi, Polyakov GV, Izokh AE (2013) Permian plume-related magmatic associations in the Song Da – Tu Le rift system and Phan Si Pan uplift, Northwest Vietnam. Extend. Abstract volume of international symposium large igneous provinces of Asia: mantle plume and metallogeny, LIPs, Hanoi, 7 Nov 2013 pp 57–61

Tran Van Tri TKT, Truong Cam Bao (eds) (1977) Geology of Vietnam, northern part. The explanation to geological map of North Vietnam, scale 1: 1.000.000. Institute of Geology and Mineral Resources (in Vietnamese)

Tran Viet Anh, Pang KN, Chung SL, Lin HM, Tran Trong Hoa, Tran Tuan Anh, Yang HJ (2011) The Song Da magmatic suite revisited: a petrologic, geochemical and Sr–Nd isotopic study on picrites, flood basalts and silicic volcanic rocks. J Asian Earth Sci 42:1341–1355

Walker RJ, Nisbet E (2002) ^{187}Os isotopic constraints on Archean mantle dynamics. Geochim Cosmochim Acta 66:3317–3325

Walker RJ, Stone W (2001) Os isotope constraints on the origin of the 2.7 Ga Boston Creek Flow, Ontario, Canada. Chem Geo 175:567–579

Walker RJ, Prichard HM, Ishiwatari A, Pimentel M (2002) The osmium isotopic composition of convecting upper mantle deduced from ophiolite chromites. Geochim Cosmochim Acta 66:329–345

Wallace PJ (1998) Water and partial melting in mantle plumes: inferences from the dissolved H2O concentrations of Hawaiian basaltic magmas. J Geophys Res Lett 25:3639–3642

Wang CY, Zhou MF, Qi L (2007) Permian flood basalts and mafic intrusions in the Jinping (SW China)–Song Da (Northern Vietnam) district: mantle sources, crustal contamination and sulfide segregation. Chem Geol 243:317–343

Xu YG, Chung SL, Jhan BM, Wu GY (2001) Petrologic and geochemical constraints on the petrogenesis of Permian-Triassic Emeishan flood basalts in South Western China. Lithos 58:145–168

Zhong H, Zhu WG, Chu ZH, He DF, Song XY (2007) Shrimp U-Pb geochronology, geochemistry, and Nd-Sr isotopic study of contrasting granites in the Emeishan large igneous province, SW China. Chem Geol 236:112–133

Zhou MF, Malpas J, Song XY, Kenedy AK, Robinson PT, Sun M, Lesher CM, Keays RR (2002) A temporal link between Emeishan large igneous province (SW China) and the end-Guadalupian mass extinction. Earth Planet Sci Lett 196:113–122

Springer
http://www.springer.com/978-3-319-25233-9

Intraplate Magmatism and Metallogeny of North
Vietnam

Tran, T.-H.; Polyakov, G.V.; Tran, T.-A.; Borisenko, A.S.;
Izokh, A.E.; Balykin, P.A.; Ngo, T.-P.; Pham, T.-D.

2016, XII, 372 p. 169 illus. in color., Hardcover
ISBN: 978-3-319-25233-9